

LIBRARY  
ROYAL AIRCRAFT ESTABLISHMENT  
BEDFORD.

R. & M. No. 2932  
(16,029)  
A.R.C. Technical Report



MINISTRY OF SUPPLY

AERONAUTICAL RESEARCH COUNCIL  
REPORTS AND MEMORANDA

# Aerodynamic Flutter Coefficients for Subsonic, Sonic and Supersonic Flow (Linear Two-dimensional Theory)

*By*

P. F. JORDAN

*Crown Copyright Reserved*

LONDON: HER MAJESTY'S STATIONERY OFFICE

1957

SIXTEEN SHILLINGS NET

# Aerodynamic Flutter Coefficients for Subsonic, Sonic and Supersonic Flow (Linear Two-dimensional Theory)

By

P. F. JORDAN

COMMUNICATED BY THE PRINCIPAL DIRECTOR OF SCIENTIFIC RESEARCH (AIR),  
MINISTRY OF SUPPLY

---

*Reports and Memoranda No. 2932\**

*April, 1953*

---

*Summary.*—The solution is derived, in a convenient form for numerical evaluation, for a two-dimensional aerofoil oscillating with arbitrary downwash at sonic speed, and is shown to be the limit of both the subsonic and the supersonic solutions as the Mach number tends to unity. Linear theory is shown to be applicable at sonic speed for an oscillating aerofoil of zero thickness, but at near-sonic speeds consideration of the lift distribution shows that linearization is not permissible. Hence for near-sonic speeds the sonic solution gives a better approximation to the non-linear solution than does the linear solution for the actual speed. It is shown that interpolation of the force coefficients is more justifiable in the subsonic range than in the supersonic range. The physical validity of the linear solution is discussed; certain singularities which occur in the transition to sonic speed are shown to have no physical significance.

The four main aerodynamic force coefficients for an oscillating two-dimensional wing are presented in the form of tables and isometric graphs over the ranges 0 to 2 of Mach number and 0 to 1.4 of frequency parameter based on the wing chord; the present sonic solution and existing subsonic and supersonic solutions have been supplemented by interpolated values for Mach numbers between 0.7 and unity.

---

1. *Introduction.*—Until recently it was the general belief that linearised aerodynamic theory was unsuitable for application at sonic and near-sonic speeds ( $M \simeq 1$ ). This belief arose from consideration of the familiar (but purely theoretical) case of a wing of infinite span, rigidly fixed right across the air stream, for which this simplified theory leads to a 'sonic barrier' of infinite lift and drag, in contradiction to its own assumption of small perturbations only. This occurrence is readily explained by the fact that the individual stream tube has its minimum cross-section at sonic speed, so that neither by acceleration nor by deceleration can way be made for the wing. However, the 'barrier' disappears if way is made for the wing by relieving the conditions of the problem, *e.g.*, by considering the wing of finite span, or the wing accelerated in the flow direction, or the oscillating wing. In all these cases—and hence in all practical cases—'reasonable,' *i.e.*, finite, forces are obtained also at sonic speed.

This observation has recently led to a number of investigations. The present paper deals with the harmonically oscillating aerofoil of zero thickness and infinite span. The fact that this problem can be linearised has been shown by Lien, Reissner and Tsien<sup>1</sup>, who have discussed the basic equations of non-steady motion. A confirmation of their conclusions is provided by the actual linear solution for the wing with rigid chord, presented graphically in Fig. 1. It appears

---

\* R.A.E. Report Structures 141, received 7th July, 1953. This report has been prepared for publication by Structures Dept., R.A.E., in the absence of the author.

that in the usual range of flutter frequencies ( $\nu > 0.2$ , say)† the order of magnitude of the solution is roughly independent of  $M$ , even in the sonic region. This agrees with the conclusions of a previous paper<sup>2</sup> that the values of the parameter 'flutter danger,' calculated for a given wing at subsonic and supersonic speeds, can usually be interpolated by smooth curves through the sonic range.

Solutions for  $M = 1$  have already been given by Heaslet, Lomax and Spreiter<sup>3</sup> and by Rott<sup>4,5</sup>. The first obtained the lift due to vertical translation by Laplace transformation of their solution of the gust problem. Rott has given formulae and numerical tables for the four main wing forces. Similar tables by Nelson and Berman<sup>6</sup> became available during the draft stage of the present report.

The present investigation was stimulated by the statement by Rott<sup>4</sup> that the sonic solution exists. As a first step the solution for  $M = 1$  is obtained (section 3.4) by an independent method‡, viz., as the limit  $M = 1 + 0$ , i.e.,  $M$  tending to unity from above. The investigation is then extended to cover the supersonic range ( $M = 1 + \delta$ ; section 3.3) and the subsonic range ( $M = 1 - \delta$ ; section 3.5). Tables and graphs covering the speed range  $0 \leq M \leq 2$  are given (section 4) and their physical validity is discussed (section 2). The main purpose of this report is thus (a) to present a new solution for sonic and near-sonic speeds, and (b) to present values of the wing force coefficients over the continuous range of Mach number (0 to 2) and frequency parameter (0 to 1.4) by combining the results of the sonic solution with values based on available results for subsonic and supersonic speeds.

Considering the limit process  $M \rightarrow 1$ , it turns out that, while the limit solution is common in its essentials to both sides (i.e., the limits  $M = 1 - 0$  and  $M = 1 + 0$  are identical to the solution for  $M = 1$ ) there is an important difference in the manner in which this limit is approached. A consequence of this difference is that interpolation of the aerodynamic coefficients both with respect to speed parameter  $M$  and to frequency parameter  $\nu$ , is better justified in the range  $M = 1 - \delta$  than in the range  $M = 1 + \delta$ . This, however, refers to the theoretical solution. From a physical point of view, and for the frequencies usual in flutter, the linear solution for  $M = 1$  should be preferred, in the near-sonic range  $M = 1 + \delta$ , to the 'correct' linear solution for the actual Mach number  $M$ .

2. *Physical Validity of the Linear Solution.*—2.1. *General Considerations.*—The presentation in this report of the linear solution for the transonic range is not meant to imply that this solution has the same degree of physical validity for the actual wing in actual flow as we are used to expect of the incompressible solution. At low speeds the oscillations are superposed on a relatively stable steady flow; experience shows that to a reasonable degree the oscillatory solution is independent of the steady disturbances, so that the unsteady solution for the infinitely thin wing can be used in flutter calculations for wings of finite thickness (provided the mean incidence is small and the frequency parameter is sufficiently large). At high speeds, and in particular at transonic speeds, the field of the steady disturbances is much less stable and highly non-linear; the degree of physical validity which may be attributed to the independent linear solution for superposed oscillations must be decided by experience.

The primary case for the application of linear theory to the transonic range is that its results, obtained with relative ease, will provide a welcome basis for the interpolation and interpretation of more reliable results which should be forthcoming from experiments and more refined theories.

---

†  $\nu = 2\pi fc/v$  is the frequency parameter, referred to chord  $c$ .

‡ Owing to its particularly simple form this solution could be used to check, and correct in one instance, the numerical tables of Ref. 5 prior to their publication. It turned out later that the limit  $M = 1 + 0$  is also considered in Refs 5 and 6.

We consider first the infinitely thin wing oscillating at zero mean incidence, for which no steady disturbance exists. The linear solution for this case is discussed below in section 3. The solution for  $M = 1$  is quite smooth (see Figs. 1, 2 and particularly 5); it thus justifies the simplifications involved in linearising the problem (provided that the frequency parameter  $\nu$  is sufficiently large) to at least the same degree as do the solutions for  $M = 0.7$  or  $M = 1.4$ , say. The same is not true if  $M$  differs slightly from unity: in the transition  $M \rightarrow 1$  singularities occur which contradict the conditions of linearisation, *i.e.*, the conditions which the solutions must fulfil in order to be valid. However, we are going to show that these singularities are a consequence of the particular (and usual) method of linearising rather than of linearisation as such, and that, as an approximation to the solution of the original, non-linear problem, the linear solution for  $M = 1$  is preferable to the linear solution for the correct value of  $M$  if  $M$  lies in a certain range  $M = 1 \pm \delta$ . How to show this is an analytical problem which is discussed in section 2.2; a few remarks concerning the physical problem, *i.e.*, the wing of finite thickness etc., follow in section 2.3.

The understanding of the subsequent discussion may be helped by anticipating section 3 in a short description of the linear near-sonic solution with the aid of Figs. 2 and 8. The perturbation field of an oscillating point disturbance in an air stream consists of long waves and short waves. The long waves do not interest us here. The length of the short waves tends to zero as  $M$  tends to unity from either side. Corresponding short waves appear in the lift distribution  $p(x)$  of the oscillating wing; at subsonic speeds, Fig. 8†, they start from the trailing edge but they start from the leading edge at supersonic speeds, Fig. 2 (in particular see the real part  $pz'$ , Fig. 2a). In Fig. 8 the local amplitude of the waves tends to zero as  $M$  tends to unity, except at the trailing edge, while in Fig. 2 it remains constant; thus  $p(x)$  has a limit for  $M = 1 - 0$  (*i.e.*, from the subsonic side, Fig. 8) but not for  $M = 1 + 0$  (*i.e.*, from the supersonic side, Fig. 2).

A different position arises if the mean local lift—see equation 3.42 (12) below—is considered. In this case both limits exist; the important points are that (a) the two limits are identical, *i.e.*, that there is a common limit, and that (b) this common limit satisfies the wave equation, thus representing the solution for  $M = 1$ .

For our subsequent discussion of the permissibility of linearisation we note that the derivative of  $p(x)$  with respect to  $x$  takes arbitrarily large values as  $M$  tends to unity from either side; that is, arbitrarily large perturbation velocities occur, not only at the leading and trailing edges—where they occur also in incompressible flow theory (owing to the simplification of the physical problem)—but at every point of the wing chord.

2.2. *Analytical Consideration of the Linear and Non-linear Problems (Two-dimensional).*—The complete non-linear differential equation for the perturbation velocity potential  $\Phi$  of a two-dimensional non-viscous flow field reads:

$$\begin{aligned} \Phi_{x'x'} \left(1 - \frac{\Phi_{x'}^2}{a^2}\right) + \Phi_{zz} \left(1 - \frac{\Phi_z^2}{a^2}\right) - \frac{2}{a^2} \Phi_{x'z} \Phi_{x'} \Phi_z \\ = \frac{1}{a^2} [\Phi_{tt} + 2\Phi_{x't} \Phi_{x't} + 2\Phi_z \Phi_{zt}] \quad \dots \quad \dots \quad \dots \quad (1) \end{aligned}$$

if  $x', z$  are Cartesian co-ordinates fixed in space,  $t$  is the time,  $a$  the local speed of sound, and suffices denote differentiation.

Let the wing proceed in the direction of the negative  $x'$ -axis and let its velocity be  $V$ . Let  $x$  be a co-ordinate fixed to the wing so that

$$x = x' + Vt \quad \dots \quad \dots \quad \dots \quad \dots \quad \dots \quad \dots \quad \dots \quad (1a)$$

† Fig. 8 shows not the lift  $p(x)$  but a function  $G(x)$  which illustrates the nature of  $p(x)$ .

and let  $\phi$  be the perturbation potential in the moving axes :

$$\phi(x, z, t) = \Phi(x', z, t) \quad \dots \quad \dots \quad \dots \quad \dots \quad \dots \quad \dots \quad \dots \quad \dots \quad \dots \quad (1b)$$

Let the perturbation velocities be  $u$  and  $w$ , so that

$$\phi_x = \Phi_{x'} = u; \quad \phi_z = \Phi_z = w \quad \dots \quad \dots \quad \dots \quad \dots \quad \dots \quad \dots \quad \dots \quad \dots \quad (1c)$$

while  $\phi_t = \Phi_t - V u$ .

Further let  $a_\infty$  be the free-stream velocity of sound and introduce

$$\bar{u} = \frac{u}{a_\infty}; \quad \bar{w} = \frac{w}{a_\infty}; \quad M = \frac{V}{a_\infty}; \quad \tau = \frac{t}{a_\infty} \quad \dots \quad \dots \quad \dots \quad \dots \quad \dots \quad (1d)$$

Assume that

$$\bar{u} \ll 1; \quad \bar{w} \ll 1 \quad \dots \quad \dots \quad \dots \quad \dots \quad \dots \quad \dots \quad \dots \quad \dots \quad (1e)$$

so that the products of  $\bar{u}$ ,  $\bar{w}$  can be neglected in comparison with unity. Transformation of (1) to the moving co-ordinates then yields

$$u_x(1 - M^2 - 2M\bar{u}) + w_z - 2Mw_x\bar{w} = \phi_{xx} + 2[u_x(M + \bar{u}) + w_x\bar{w}]. \quad (2)$$

Equation (2) is linear in incompressible flow ( $a_\infty = \infty$ ) but is non-linear in compressible flow. The familiar linear equation for the latter case is obtained if all the remaining non-linear terms in (2) are also neglected, *i.e.*, if

$$\bar{u} = \bar{w} = 0 \quad \dots \quad \dots \quad \dots \quad \dots \quad \dots \quad \dots \quad \dots \quad \dots \quad (2a)$$

is formally introduced in (2).

Consider in particular the transonic range. Let  $M = 1 + \delta$  and let

$$\delta \ll 1. \quad \dots \quad \dots \quad \dots \quad \dots \quad \dots \quad \dots \quad \dots \quad \dots \quad (3)$$

Assume harmonic motion ; let  $2\pi f$  be the circular frequency. Further let the co-ordinates  $x$  and  $z$  be made non-dimensional with some length  $c$  as reference length. Then (2), after multiplication by  $c$ , becomes

$$- 2u_x(\delta + \bar{u}) + w_z - 2w_x\bar{w} = - \frac{1}{c} v_0^2 \phi + 2iv_0[u(1 + \delta + \bar{u}) + w\bar{w}] \quad \dots \quad (4)$$

if

$$v_0 = 2\pi fc/a_\infty$$

is the frequency parameter referred to  $c$  and the free-stream speed of sound.

The conditions which the solution of the linear problem (2a), (4) must fulfil in order that (2a) is justified can be deduced from (4) :

(a)  $\bar{u}$ ,  $\bar{w}$ , if related to the wing amplitudes, must be of the same order as in the solution for  $M = 0$ , say

(b)  $u_x$ ,  $w_x$  must be of order  $v_0 u$ ,  $v_0 w$

Further, as  $\delta$  appears in (4) in the combination  $(\delta + \bar{u})$  only, a consequence of (a) and (b) will be

(c) the parameter  $M$  has negligible effect.

In fact the solution of (4), (2a), described in section 2.1 with the aid of Figs. 2 and 8, fulfils neither condition (b) nor (c) :  $u_x$  takes arbitrarily large values if  $\delta$  is sufficiently near to zero. Has the conclusion to be drawn that linearisation is not permissible in the transonic range ?

The existence of the regular solution for  $M = 1$  contradicts this conclusion; it can rather be argued that, as the non-linear equation (4) describes a physical problem, the solution of (4) for  $M = 1 \pm \delta$  cannot be far different from the linear solution for  $M = 1$ . Indeed if (1e) justifies (2a) then (3) justifies

$$\bar{u} + \delta = \bar{w} = 0. \quad \dots \dots \dots \dots \dots \dots \dots \dots \dots \dots \quad (4a)$$

Equations (4), (4a) define an alternative linear problem in which  $M$  no longer appears; the solutions of (4), (4a) fulfil the conditions (a) to (c), thus justifying the assumptions made. Hence the linear solution for  $M = 1$  can be accepted as a reasonable approximation throughout that near-sonic range where the usual linear solution does not fulfil condition (b)†.

2.3. *Application to Actual Wings.*—The argument of section 2.2 is reassuring as regards the physical validity of linear theory in the sonic range—reassuring in so far as the non-linear solution for the thin plate at zero mean incidence can be accepted as the solution for the actual wing. Reassuring also is an ‘analytic result of G. L. Sewell which indicated that the presence of attached shock waves had no effect on the end result of the small disturbance, non-steady, potential theory at low supersonic speed’ (stated by Garrick<sup>8</sup>). On the other hand W. P. Jones<sup>9</sup> has shown that the thickness effect is not negligible. He investigated the range  $M \geq 1.4$ , but his conclusions should also apply if  $M \simeq 1$ .

A serious objection to the application of two-dimensional theory to wings of finite span at near-sonic speeds arises from the fact that the spanwise co-ordinate attains major importance as  $M$  tends to unity, the effective aspect ratio being

$$A_c = \sqrt{\{1 - M^2\}}A.$$

Further, the three-dimensional sonic lift distribution is quasi-subsonic in that upper and lower wing surfaces are interdependent (for all wing shapes), while the two-dimensional distribution is quasi-supersonic in this respect; on the other hand the leading-edge singularity of the latter is already quasi-subsonic, see Fig. 2, so that the two distributions have the same form at both leading and trailing edges, provided that the trailing edge is normal to the air stream. The quantitative effect of these points requires further investigation.

Flutter speeds calculated from a self-contained set of theoretical aerodynamic derivatives are often in better agreement with experiment than are the derivatives themselves. This may be why the little evidence that is available from transonic flight tests seems to indicate that flutter calculations based on linear derivatives show the correct tendency. No experimental results at near-sonic speeds exist for comparison with the theoretical result, given here. However, the wind-tunnel flutter tests by Tuovila, Baker and Regier<sup>10</sup> at low supersonic speeds ( $M = 1.3$ ) should be mentioned as giving some confirmation of linear theory. On the other hand the measurements of damping in pitch by Bratt and Chinneck<sup>11</sup> ( $M \geq 1.275$ ) are sometimes quoted as a refutation of linear theory: in these experiments positive damping was found instead of the negative damping predicted by theory. However, the pitching centre in these tests was at mid-chord and was thus near the border of the predicted range of negative damping, Fig. 3. Thus the expected inaccuracy‡ rather than a failure of the theory was shown. Further, the frequency parameter value of the test was very small ( $\nu < 0.03$ ) so that damping due to boundary-layer effects can be assumed to have been larger than it would have been in the usual frequency range of flutter.

---

†A similar practice prevails in another of the cases mentioned in section 1, *viz.*, in the case of the steady wing of finite aspect ratio. Here the effect of  $\delta$  is accepted to be negligible for a wing of aspect ratio  $A$  if

$$\delta A^2 \ll 1$$

—in spite of the fact that the lift-slope curve as obtained by linear theory has a vertical tangent for  $M = 1 + 0$ .

‡Due largely to the finite thickness of the wing model; see W. P. Jones<sup>9</sup>.

3. *Linear Analysis for the Thin Aerofoil Oscillating Harmonically in Two Dimensional Flow.*—  
 3.1. *Introductory Remarks.*—The present section is concerned with the purely mathematical task of solving the two-dimensional linearised problem of the thin aerofoil at zero mean incidence oscillating harmonically with an arbitrary mode  $z(x)$  in non-viscous flow, and in particular with the transition  $M \rightarrow 1$  both from the supersonic side and from the subsonic side. The fundamental equation governing the lift distribution  $p(x)$  along the chord will in both cases be used in its integral form rather than in the equivalent differential form (2a), (4) of section 2.2.

The total wing forces as shown in Fig. 1 appear to be regular functions of  $\nu$  and  $M$  if the neighbourhood of the point  $[\nu, M] = [0, 1]$  is excluded. This gives a wrong impression of the difficulties of the problem and is due partly to the fact that not all the details of the transition  $M \rightarrow 1$  can be shown in these drawings, and partly to the fact that total forces are considered. A better insight into the difficulties of the problem is obtained from Fig. 4, where 'standard lift distributions'  $p_0(x)$  are shown. These are defined, for a given speed  $M$ , as

$$p_0(x) = \lim_{\nu \rightarrow 0} \left( \frac{p(x, \nu)}{p(0.5, \nu)} \right) \quad \dots \quad \dots \quad \dots \quad \dots \quad \dots \quad \dots \quad \dots \quad (1)$$

$p(x, \nu)$  being the lift distribution due to pitch.

There are only three different distributions  $p_0(x)$  :

$$p_0(x) = \left\{ \begin{array}{l} \sqrt{(1-x)/x} \\ 1/\sqrt{(2x)} \\ 1 \end{array} \right\};$$

$$x_0 = \left\{ \begin{array}{l} \frac{1}{4} \\ \frac{1}{3} \\ \frac{1}{2} \end{array} \right\} \text{ if } M \left\{ \begin{array}{l} < 1 \text{ subsonic} \\ = 1 \text{ sonic} \\ > 1 \text{ supersonic} \end{array} \right\} \quad \dots \quad \dots \quad \dots \quad \dots \quad (1a)$$

( $x_0$  is the position of the centre of pressure of  $p_0(x)$ .)

The subsonic distribution is characterised by its singularities of order  $1/\sqrt{x}$  at the leading edge and  $\sqrt{x}$  at the trailing edge; the supersonic distribution exhibits neither singularity. The sonic distribution is quasi-subsonic at the leading edge but is quasi-supersonic at the trailing edge. This distinction is still valid if  $\nu$  is not zero, *see, e.g.*, Fig. 2. It follows that the transition  $M \rightarrow 1$  is irregular and non-uniform whether the sonic speed is approached from below or from above.

Our analytical method is to replace the cylinder functions in the fundamental equations by asymptotic expressions. These expressions are useful if their argument is sufficiently large. This argument being  $\nu/|1 - M^2|$ , our investigation applies to a part of the  $\nu, M$ -plane which contains the sonic line  $M = 1$  and has an apex at the point  $[\nu, M] = [0, 1]$ .

3.2. *Notation.*—(a) *General*

- $\rho$       Air density
- $V$       Speed of wing
- $M$       Free-stream Mach number
- $\gamma = 1/M$  Reciprocal Mach number





If  $n = 1, 2, 3 \dots$  then

$$\bar{n}! = \sqrt{\pi} \cdot \frac{1}{2} \cdot \frac{3}{2} \dots \frac{2n-1}{2}; \quad \overline{-n}! = \pi(-)^n / \bar{n}!$$

$$\bar{\bar{n}} = \sqrt{\pi} \cdot \frac{1}{2} \cdot \frac{3}{4} \dots \frac{2n-1}{2n}; \quad \overline{-\bar{n}} = 0.$$

If  $n \gg 1$ , then

$$\bar{n}! \simeq \frac{n!}{\sqrt{n}}; \quad \bar{\bar{n}} \simeq \frac{1}{\sqrt{n}}$$

$n$	-2	-1	0	1	2	3	4
$n!$	$\infty$	$\infty$	1	1	2	6	24
$\bar{n}!/\sqrt{\pi}$	4/3	-2	1	1/2	3/4	15/8	105/16
$\bar{\bar{n}}/\sqrt{\pi}$	0	0	1	1/2	3/8	5/16	35/128

3.3. *Supersonic Wing Force Coefficients* ( $M = 1 + \delta$ ).—Two-dimensional linear supersonic theory has been discussed by numerous authors; see, e.g., Refs. 7, 12 and 13. As a result, the four force coefficients of the wing with rigid chord, defined in section 3.2(b), may be written in the form

$$l_x = 2\omega^2 H + 2\omega(K_0 - K_1)$$

$$l_a = \left(1 + \frac{1}{\omega}\right) l_x + m_x$$

$$-m_x = (\omega^2 - 1 + \kappa)H + (\omega + 1)(K_0 - K_1) - \kappa K_0$$

$$-m_a = \left[\frac{1}{\omega}(1 - \kappa) + \omega + \frac{2}{3}\omega^2\right]H + \left[\frac{1}{3}(2\omega + 1) - \frac{1}{\omega}(1 - \kappa)\right](K_0 - K_1)$$

$$+ \frac{\kappa}{3}\left(2K_0 + \frac{1}{\omega}K_1\right). \quad \dots \quad \dots \quad \dots \quad \dots \quad \dots \quad \dots \quad \dots \quad (1)$$

Here

$$H \equiv H(\gamma, \nu) = \frac{\gamma}{\sqrt{\kappa}} \int_0^1 J_0\left(\frac{\gamma\nu}{\kappa} \xi\right) e^{-\omega\xi/\kappa} d\xi$$

$$K_p \equiv K_p(\gamma, \nu) = \frac{\gamma}{\sqrt{\kappa}} (-i\gamma)^p e^{-\omega/\kappa} J_p\left(\frac{\gamma\nu}{\kappa}\right), \quad \dots \quad \dots \quad \dots \quad \dots \quad (1a)$$

$\omega = i\nu$  is the imaginary frequency parameter and

$$\gamma = 1/M < 1; \quad \kappa = 1 - \gamma^2 > 0 \quad \dots \quad \dots \quad \dots \quad \dots \quad \dots \quad (1b)$$

are speed parameters.  $J_p$  are Bessel functions of the first kind.

The function  $H$  may be transformed into

$$H = -\gamma \left[ \frac{i}{\nu} + \frac{1}{\sqrt{\kappa}} \int_1^{\infty} e^{-\omega\xi/\kappa} J_0\left(\frac{\gamma\nu}{\kappa} \xi\right) d\xi \right] \quad \dots \quad (1c)$$

by means of Schwarz<sup>14</sup>, equation (46).

We are concerned with the range  $\nu/\kappa \gg 1$ . The functions  $H$  and  $K_p$  may therefore be evaluated by using asymptotic expressions for the Bessel functions (see equation AI(1)†). For  $K_p$  we obtain immediately

$$K_p \sim \frac{\gamma^{p+0.5}}{\pi} \frac{1}{(2\pi\omega)^{0.5}} \sum_0^{\infty} \frac{\overline{m+p!} \overline{m-p!}}{m!} \left(\frac{\kappa}{2\gamma\omega}\right)^m \left\{ e^{-u} + i(-)^{m+p} e^{-v} \right\} \quad \dots \quad (2)$$

with

$$\left. \begin{aligned} u &= \frac{\omega}{1+\gamma} \rightarrow \frac{\omega}{2} \\ v &= \frac{\omega}{1-\gamma} \rightarrow i\infty \end{aligned} \right\} \text{if } M \rightarrow 1. \quad \dots \quad (2a)$$

Some further transformations are required in the case of the function  $H$ . Substituting AI(1) in (1c) yields

$$H \sim \gamma \left\{ \frac{1}{\omega} - \frac{1}{\pi(2\pi\omega\gamma)^{0.5}} \sum_0^{\infty} \overline{m} \left(\frac{\kappa}{2\omega\gamma}\right)^m [I_m(u) + i(-)^m I_m(v)] \right\} \quad \dots \quad (3)$$

where

$$I_m(\alpha) \equiv \overline{m!} \int_1^{\infty} \frac{e^{-\alpha\xi}}{\xi^{m+0.5}} d\xi. \quad \dots \quad (3a)$$

The two cases  $I_m(u)$  and  $I_m(v)$  have to be treated differently in view of the limit  $M \rightarrow 1$  (see 2a)). Applying the relation

$$I_m(\alpha) = \overline{m-1!} e^{-\alpha} - \alpha I_{m-1}(\alpha) \quad \dots \quad (3b)$$

in opposite directions we obtain

$$I_m(u) = (-u)^m \left[ I_0(u) + e^{-u} \sum_1^m \frac{\overline{n-1!}}{(-u)^n} \right] \quad \dots \quad (4a)$$

$$I_m(v) \sim -(-v)^m e^{-v} \sum_{m+1}^{\infty} \frac{\overline{n-1!}}{(-v)^n}. \quad \dots \quad (4b)$$

(4b) is an asymptotic expansion of a well known type‡.  $I_0(u)$  is essentially a Fresnel integral. Introduce (see AI(2))

$$U = \pi \sqrt{\left\{ \frac{2\gamma}{1+\gamma} \right\}} \sum_0^{\infty} \frac{(-u)^n}{n!(n+0.5)} = \pi \sqrt{\left\{ \frac{\gamma\pi}{v} \right\}} F\left(\frac{v}{1+\gamma}\right). \quad \dots \quad (5)$$

Then

$$I_0(u) = \overline{0!} \left( \int_0^{\infty} - \int_0^1 \right) \frac{d\xi}{\sqrt{\xi}} e^{-u\xi} = \pi u^{-0.5} - \sqrt{\left\{ \frac{1+\gamma}{2\pi\gamma} \right\}} U. \quad \dots \quad (5a)$$

† AI refers to the Appendix I.

‡ See, e.g., Copson<sup>15</sup> p. 231.

Owing to AI(3a)

$$I_0(u) \sum_0^{\infty} \bar{m} \left( \frac{-u\kappa}{2\omega\gamma} \right)^m = \pi \sqrt{\left( \frac{2\pi\gamma}{\omega} \right)} - U \dots \dots \dots \dots \dots \quad (5b)$$

The term  $1/\omega$  in (3) is cancelled if (4a) and (5b) are introduced. Introducing also (4b) and changing the order of summation we obtain finally

$$H \sim \frac{\sqrt{\gamma}}{\pi(2\pi\omega)^{0.5}} \left\{ U - \sum_1^{\infty} \frac{\overline{n-1}!}{(-\omega)^n} \left[ (1+\gamma)^n e^{-u} \sum_n^{\infty} \bar{m} \left( \frac{\gamma-1}{2\gamma} \right)^m \right. \right. \\ \left. \left. - i(1-\gamma)^n e^{-v} \sum_0^{n-1} \bar{m} \left( \frac{1+\gamma}{2\gamma} \right)^m \right] \right\} \dots \dots \dots \dots \dots \quad (6)$$

Substituting (2) and (6) in (1) yields the complete asymptotic expansions for the four wing force coefficients.

Consider in particular the transition  $M \rightarrow 1$ . The functions  $U$  and  $\exp(-u)$  are regular; however, this is not true of the function  $\exp(-v)$ , which represents a waveform whose wavelength becomes smaller and smaller as  $M$  tends to unity—compare (2a). Fortunately  $\exp(-v)$  has the factor  $1-\gamma \simeq M-1 \simeq \frac{1}{2}\kappa \rightarrow 0$  in all four coefficients (1) (this is immediately seen for  $H$  from (6) and is seen for the function  $K_p$  if the difference  $K_0 - K_1$  is formed). Thus the four coefficients are regular in  $M \geq 1$ ; however their derivatives with respect to  $M$  are not regular†.

3.4. *Sonic Speed* ( $M = 1 + 0$ ).—3.4.1. *Wing force coefficients*.—Introducing  $\gamma = 1$  in 3.3(2), (6), we obtain

$$H = \frac{2}{(2\pi\omega)^{0.5}} \sum_0^{\infty} \left( -\frac{\omega}{2} \right)^n \frac{1}{n!(2n+1)} \dots \dots \dots \dots \dots \quad (1)$$

$$K_0 - K_1 = \frac{2}{(2\pi\omega)^{0.5}} \sum_0^{\infty} \left( -\frac{\omega}{2} \right)^n \frac{1}{n!} \dots \dots \dots \dots \dots \quad (1)$$

We write the four wing force coefficients as series of similar form

$$l_x = \frac{8}{(2\pi\omega)^{0.5}} \sum_0^{\infty} \left( -\frac{\omega}{2} \right)^n l_x^n \dots \dots \dots \dots \dots \quad (2)$$

From (1), (2) and 3.3(1)

$$l_x^n = \frac{1}{(n-1)!(2n-3)}; \quad l_x^0 = 0 \dots \dots \dots \dots \dots \quad (2a)$$

and

$$\left. \begin{aligned} l_a^n &= \frac{2}{2n+1} l_x^n - \frac{1}{2} l_x^{n+1} \\ -m_x^n &= \frac{2n-1}{2n+1} l_x^n \\ -m_a^n &= \frac{2n+1}{2n+3} l_a^n \end{aligned} \right\} \dots \dots \dots \dots \dots \quad (2b)$$

† See section 3.3.2.

The series (2) converge for all values  $\nu$ ; they converge rapidly in the usual range of flutter frequencies, where numerical evaluation is convenient owing to the simple form of the series coefficients. Numerical values are contained in Tables 2 and 3.

It should be noted here that, while the simplicity of (2a) is of course a peculiarity of the sonic solution, the relations (2b) represent, in their essence, a property of the whole range  $M \geq 1$ .†

Expanding (2), (2a), (2b) we obtain

$$\left. \begin{aligned} l_z &= \frac{1-i}{\sqrt{(\pi\nu)}} (0 + 2i\nu - \nu^2 \dots) \\ l_a &= \frac{1-i}{\sqrt{(\pi\nu)}} \left( 2 + \frac{7}{3}i\nu - \frac{19}{60}\nu^2 \dots \right) \\ -m_z &= \frac{1-i}{\sqrt{(\pi\nu)}} \left( 0 + \frac{2}{3}i\nu - \frac{3}{5}\nu^2 \dots \right) \\ -m_a &= \frac{1-i}{\sqrt{(\pi\nu)}} \left( \frac{2}{3} + \frac{7}{5}i\nu - \frac{19}{84}\nu^2 \dots \right) \end{aligned} \right\} \dots \dots \dots \dots \dots \quad (4)$$

Both in translation and pitch the first non-zero term represents a force which has its centre of pressure at  $x_0 = 1/3$ . In each case let suffix  $s$  denote the  $s$ th non-zero term; from (2b)

$$x_{0,s} = \frac{2s-1}{2s+1} \quad (M=1) \dots \dots \dots \dots \dots \quad (5)$$

The corresponding supersonic relation is from (3a)

$$x_{0,s} = \frac{s}{s+1} \quad (M > 1) \dots \dots \dots \dots \dots \quad (5a)$$

In all cases

$$\lim_{s \rightarrow \infty} x_{0,s} = 1.$$

† In the supersonic range we may write

$$l_z = \sum_0^{\infty} \left( -\frac{\omega}{2} \right)^m l_z^m \dots \dots \dots \dots \dots \quad (3)$$

The series (3) converge if  $\nu/\kappa < 2$ . The relations corresponding to (2b) are

$$\left. \begin{aligned} l_a^m &= \frac{1}{m+1} l_z^m - \frac{1}{2} l_z^{m+1} \\ -\vec{m}_z^m &= \frac{m}{m+1} l_z^m \\ -\vec{m}_a^m &= \frac{m+1}{m+2} l_a^m \end{aligned} \right\} \dots \dots \dots \dots \dots \quad (3a)$$

see Jordan<sup>13</sup> (31) to (33). Now the coefficients  $l_z^m \dots$  belong to the power  $m$  of  $\omega$  while the coefficients  $l_z^n \dots$  belong to the power  $(n - 0.5)$  in (2). Accordingly (3a) becomes (2b) if  $m$  is replaced by  $(n - 0.5)$ .

3.4.2. *Lift distributions.*—The basic formula connecting lift distribution  $p(x)$  and downwash  $w(x)$  in supersonic flow may be written

$$p(x) = \frac{2\gamma}{\sqrt{\kappa}} \left\{ \int_0^x [w'(x - \xi) + w(x - \xi)] e^{-\omega\xi/\kappa} J_0\left(\frac{\gamma\nu}{\kappa} \xi\right) d\xi + w(0) e^{-\omega x/\kappa} J_0\left(\frac{\gamma\nu}{\kappa} x\right) \right\} \dots \dots \dots \dots \quad (6)$$

—see Ref. 12 equation (43)—provided that  $w(x)$  is continuous for  $0 < x < 1$ . We require the limit of  $p(x)$  as  $M$  tends to unity. The formal procedure of inserting the asymptotic expression AI(1) in (6) and then letting  $M$  tend to unity yields the correct limit for  $p(x)$  in spite of the fact that the argument of  $J_0$  reaches zero in the integral. This may be proved by dividing the range  $[0, x]$  of the integral into the two ranges  $[0, \sqrt{\kappa}]$ , and  $[\sqrt{\kappa}, x]$ . The integral over the first range disappears as  $\kappa$  tends to zero. In the second range insert AI(1). Thus an error is committed which depends on the lower limit of the argument of  $J_0$ , *viz.*, on  $\gamma\nu/\sqrt{\kappa}$ ; as  $\kappa$  tends to zero, this lower limit tends to infinity and the error vanishes.

The supersonic lift distribution  $p(x)$  is independent of the chord length  $c$ ; hence we introduce a modified chordwise co-ordinate

$$\hat{x} = \frac{\pi c x}{V/f} = \frac{1}{2} \nu x \quad \dots \quad \dots \quad \dots \quad \dots \quad \dots \quad \dots \quad \dots \quad \dots \quad \dots \quad (7)$$

referring the physical co-ordinate  $cx$  to the wavelength  $V/f$ , and further

$$y = i\hat{x} = \frac{1}{2} \omega x \quad \dots \quad \dots \quad \dots \quad \dots \quad \dots \quad \dots \quad \dots \quad \dots \quad \dots \quad (7a)$$

Thus

$$\lim_{\gamma \rightarrow 1} \frac{2\gamma}{\sqrt{\kappa}} e^{-\omega x/\kappa} J_0\left(\frac{\gamma\nu}{\kappa} x\right) = \frac{1}{(\pi y)^{0.5}} \{e^{-y} + iT(y)\} \quad \dots \quad \dots \quad \dots \quad (8)$$

where

$$T(y) = \lim_{\gamma \rightarrow 1} e^{2y/(\gamma-1)} \quad \dots \quad \dots \quad \dots \quad \dots \quad \dots \quad \dots \quad \dots \quad \dots \quad \dots \quad (8a)$$

The downwash  $w(x)$  arises from the mode  $z(x)$  and is given by

$$w(x) = z_x(x) + \omega z(x) \quad \dots \quad \dots \quad \dots \quad \dots \quad \dots \quad \dots \quad \dots \quad \dots \quad \dots \quad (9)$$

We consider the elementary downwash distribution

$$w_r(x) \equiv w_r \equiv y^r (r \geq 0) \quad \dots \quad \dots \quad \dots \quad \dots \quad \dots \quad \dots \quad \dots \quad \dots \quad \dots \quad (9a)$$

where  $r$  is positive or zero but need not be integral.

The lift distribution arising from  $w_r$  we denote by

$$p_r \equiv p_r(x) \quad \dots \quad \dots \quad \dots \quad \dots \quad \dots \quad \dots \quad \dots \quad \dots \quad \dots \quad (9b)$$

When (8) is substituted in (6), that part of the integral which contains  $T(\eta)$  disappears owing to the Riemann-Lebesgue lemma. Thus (6) becomes

$$p_r = \frac{1}{\sqrt{\pi}} \left\{ \int_0^y [r + 2(y - \eta)] (y - \eta)^{r-1} e^{-\eta} \eta^{-0.5} d\eta + w(0) e^{-y} y^{-0.5} [1 + ie^y T(y)] \right\} \quad \dots \quad \dots \quad \dots \quad (10)$$

Consider first the case  $r > 0$ . As  $w(0) = 0$ , the awkward term  $T(y)$  disappears, and we obtain by means of AI(5b)

$$p_r = \frac{r!}{\sqrt{\pi}} \sum_{n=0}^{\infty} \bar{n} (-y)^n \left\{ \frac{1}{r+n!} + \frac{2y}{r+n+1!} \right\} y^{r-0.5} \quad \dots \quad \dots \quad \dots \quad (10a)$$

or

$$p_r = \frac{r!w_r}{(\pi y)^{0.5}} \sum_{n=0}^{\infty} \bar{n} \frac{(-y)^n}{r+n!} \frac{1+2n}{1-2n} \quad \dots \quad \dots \quad \dots \quad \dots \quad (11)$$

This is the final result. The series (11) converges for any value  $y$ ; it converges rapidly in the range required for flutter calculations.

We have still to consider the case  $r = 0$ ,  $w_0 \equiv 1$ . The function  $T(y)$  is represented graphically by a wave-form of zero wavelength—this means that the real and imaginary parts of  $p_0$  are both represented not by single curves but by strips of width  $\sqrt{(2/\pi\hat{x})}$ . (In other words, the transition  $M \rightarrow 1$  is not regular; the physical significance of this fact has been discussed in section 2.) However, the ambiguity which is thus introduced is eliminated by defining  $p(x)$  to be the mean lift on a finite length of wing chord:

replace  $p(x)$  by  $\lim_{\epsilon \rightarrow 0} \frac{1}{2\epsilon} \int_{x-\epsilon}^{x+\epsilon} p(x) dx \quad \dots \quad \dots \quad \dots \quad \dots \quad \dots \quad (12)$

By means of the operation (12),  $T(y)$  disappears in (10) which is otherwise left intact. It is then easily shown that application of AI(5b) to the case  $r = 0$  again leads to (11). Thus (11) is valid for  $r \geq 0$ .

By superposition of the elementary solutions (11) the lift distribution caused by any downwash distribution  $w(x)$  which may occur on a wing with rigid or non-rigid chord can be obtained.

Equation (11) connects downwash  $w$  and lift  $p$  by means of a kind of response function which depends on the power  $r$ :

$$p_r = (\bar{y})^{0.5} P_r w_r \quad \dots \quad \dots \quad \dots \quad \dots \quad \dots \quad \dots \quad \dots \quad (13)$$

Sample response functions  $P_r = P_r' + iP_r''$  are shown in Fig. 5. The fact that the curves of Fig. 5 are perfectly regular and smooth supports the argument of section 2. It is easy to show that

$$P_r' \rightarrow r; \quad P_r'' \rightarrow \frac{3\hat{x}}{2\sqrt{r}} (r \rightarrow \infty) \quad \dots \quad \dots \quad \dots \quad \dots \quad \dots \quad \dots \quad (13a)$$

3.4.3. *Comparison of results.*—The downwash distributions due to unit vertical translation (suffix  $z$ ) and to unit pitch (suffix  $\alpha$ ) about the leading edge are, owing to 3.4.2(9), (9a)

$$w_z = \omega w_0 \quad (z = 1)$$

$$w_\alpha = \dot{w}_0 + 2w_1 \quad (z = x)$$

and hence the corresponding lift distributions are

$$\begin{aligned} p_z &= \omega p_0 \\ p_\alpha &= p_0 + 2p_1 \end{aligned} \quad \left( p_z \text{ and } p_\alpha \text{ are shown in Fig. 2} \right).$$

Thus the four main wing force coefficients are :

$$\left. \begin{aligned}
 l_z &= \int_0^1 p_x dx = 2 \int_0^{\omega/2} p_0 dy \\
 l_a &= \int_0^1 p_a dx = \frac{1}{\omega} l_z + \frac{4}{\omega} \int_0^{\omega/2} p_1 dy \\
 -m_z &= \int_0^1 x p_x dx = \frac{4}{\omega} \int_0^{\omega/2} y p_0 dy \\
 -m_a &= \int_0^1 x p_a dx = -\frac{1}{\omega} m_z + \frac{8}{\omega^2} \int_0^{\omega/2} y p_1 dy
 \end{aligned} \right\} \dots \dots \dots (14)$$

Substituting 3.4.2 (11) in (14) leads again to 3.4.1(2), (2a), (2b).

3.4.4. *Control surfaces.*—In linear theory the specific property of supersonic flow that no disturbance produces any effect upstream is still valid at sonic speed. (As a consequence all force coefficients required for the flutter calculation of a wing with control surfaces are linear combinations† of the four main wing force coefficients (see 3.4.1(2) and Tables 2 and 3). When the control-surface coefficients for  $M = 1$  have been obtained in this way approximate values for high subsonic speeds can be obtained by interpolation§ (see sections 3.5.4 and 4.1).

3.5. *Subsonic Range* ( $M = 1 - \delta$ ).—In the subsonic range the lift distribution  $p(x)$  is the solution of the Possio equation (see, e.g., Ref. 17)

$$w(x) = v \int_0^1 k[v(x - \xi)] p(\xi) d\xi. \quad \dots \dots \dots (1)$$

The symbol \*j denotes Cauchy's principal value. The kernel  $k[v(x - \xi)]$  of the integral equation (1) has the form

$$k(\mathbf{x}) = \frac{\sqrt{(1 - M^2)}}{2\pi \mathbf{x}} - i \frac{\log |\mathbf{x}|}{2\pi \sqrt{(1 - M^2)}} + \dots \dots \dots (1a)$$

In (1a) the argument  $v(x - \xi)$  is replaced by  $\mathbf{x}$  for shortness. Owing to the singularity of order  $\mathbf{x}^{-1}$  of the kernel the integral equation (1) has a continuum of solutions  $p(\mathbf{x})$ ; a unique solution is enforced by adding to (1) the Kutta-Joukowski condition

$$p(1) < \infty. \quad \dots \dots \dots (1b)$$

To the speed parameters 3.3(1b) for the supersonic range correspond the parameters

$$M < 1; \quad \kappa = 1 - M^2 > 0 \dots \dots \dots (2)$$

for the subsonic range.

† e.g., the oscillating aileron behind a steady wing can be treated as a free wing; the force on the aileron due to wing motion is obtained by deducting from the total wing force the force on the front part of the wing. A complete table of the coefficients required for the wing with aileron and tab, both with aerodynamic balance, is given in Ref. 13.

§ For extensive tables of control-surface coefficients up to  $M = 0.7$ , see Minhinnick<sup>16</sup>.

3.5.1. *Possio kernel*.—The kernel  $k(\mathbf{x})$  of 3.5 (1), though regular for  $|\mathbf{x}| > 0$ , is a fairly complicated function† of its parameters  $\mathbf{x}$  and  $M$ . An asymptotic expression for  $k(\mathbf{x})$  is developed in Appendix III; the result is

$$\left. \begin{aligned} k(\mathbf{x}) &\sim K\left(\frac{2\mathbf{x}}{1+M}\right) \exp\left(i\frac{1-M}{1+M}\mathbf{x}\right) - \left(\frac{i}{2\mathbf{x}}\right)^{0.5} \sum_{n=1}^{\infty} \left(\frac{i\mathbf{x}}{2M\mathbf{x}}\right)^n C_n \exp\left(-\frac{iM\mathbf{x}}{1+M}\right) \\ k(-\mathbf{x}) &\sim \left(\frac{i}{2\mathbf{x}}\right)^{0.5} \sum_{n=1}^{\infty} \left(\frac{i\mathbf{x}}{2M\mathbf{x}}\right)^n D_n \exp\left(-\frac{iM\mathbf{x}}{1-M}\right) \end{aligned} \right\} \quad (3)$$

if

$$\mathbf{x} > 0 \quad \dots \quad \dots \quad \dots \quad \dots \quad \dots \quad \dots \quad \dots \quad \dots \quad \dots \quad (3a)$$

and

$$K(\mathbf{x}) = \left(\frac{i}{2\mathbf{x}}\right)^{0.5} e^{-i\mathbf{x}/2} \sum_0^{\infty} \frac{1}{n!} \left(-\frac{i\mathbf{x}}{2}\right)^n \quad \dots \quad \dots \quad \dots \quad \dots \quad \dots \quad (3b)$$

The coefficients  $C_n, D_n$  are given by AIII (12a), (13a); in particular

$$\lim_{M \rightarrow 1} 2nC_n = \lim_{M \rightarrow 1} D_n = \frac{\overline{n-1}}{\sqrt{\pi}} \cdot \frac{\overline{n}}{\pi} \quad \dots \quad \dots \quad \dots \quad \dots \quad \dots \quad (3c)$$

Thus

$$\lim_{M \rightarrow 1} \begin{cases} k(\mathbf{x}) = K(\mathbf{x}) \\ k(-\mathbf{x}) = 0 \end{cases} \quad \dots \quad \dots \quad \dots \quad \dots \quad \dots \quad \dots \quad \dots \quad (4)$$

It appears that the kernel  $k(\mathbf{x})$  loses an important feature during the transition  $M \rightarrow 1$ : the limit function  $K(\mathbf{x})$  is integrable throughout.

$k(\mathbf{x})$  is shown graphically‡ in Fig. 6 ( $k \equiv k' + ik''$ ).

3.5.2. *Solution for  $M = 1 - 0$* .—In the limit  $M = 1 - 0$  the Possio equation 3.5(1), owing to 3.5.1(4), becomes

$$w(x) = \nu \int_0^x K(\nu\xi) \phi(x - \xi) d\xi \quad \dots \quad \dots \quad \dots \quad \dots \quad \dots \quad (5)$$

Consider the elementary downwash  $w_r$ , see 3.4.2(9). Inserting 3.5.1(3b) in (5) and making use 3.4.2(7), (9b) we obtain

$$w_r \equiv y^r = \int_0^y e^{-\eta} \eta^{-0.5} d\eta \phi_r(y - \eta) \sum_0^{\infty} \frac{(-\eta)^m}{m!} \quad \dots \quad \dots \quad \dots \quad \dots \quad (6)$$

We are going to show that 3.4.2(11), the lift distribution for  $M = 1 + 0$ , is also the solution of (6), *i.e.*, the lift distribution for  $M = 1 - 0$ . For this purpose transform 3.4.2(10a) by means of AI(4c):

$$\phi_r = y^{r-0.5} e^{-y} \sum_0^{\infty} \frac{y^n}{n!} \{r \cdot \overline{n+r-0.5} + 2y \cdot \overline{n+r+0.5}\}$$

†Owing to this complexity no closed form solution—as exists for  $M = 0$  and  $M \geq 1$ —has yet been found for  $0 < M < 1$ .

‡The numerical values of the kernel for  $M < 1$  are taken from the tables of Schwarz and Schade<sup>18</sup>. Numerical values for  $M = 1$  are given in Table 6.



or†

$$p_r = y^{r-0.5} e^{-y} \sum_0^{\infty} \frac{y^n}{n! n+r} \frac{2n+r}{n+r} \dots \dots \dots \dots \dots \dots \quad (7)$$

Denote by  $R(y)$  the right-hand side of (6) after (7) has been inserted in it ; thus

$$R(y) = e^{-y} \int_0^y \frac{d\eta}{[\eta(y-\eta)]^{0.5}} \sum_{m=0}^{\infty} \frac{(-\eta)^m}{m!} \sum_{n=0}^{\infty} \frac{(y-\eta)^{n+r}}{n+r!} \frac{(n+r)!}{n!} \frac{2n+r}{n+r} \dots \quad (8)$$

Apply AI(5a) with  $n+r$  for  $p$ ,  $m+n+r$  for  $q$ , and  $t$  for  $m+n$ .

$$\text{Thus } R(y) = y^r e^{-y} \sum_{t=0}^{\infty} \frac{(-y)^t}{(t+r)!} S(t) \dots \dots \dots \dots \dots \dots \quad (9)$$

where

$$S(t) = \sum_{n=0}^t (-)^n \frac{(n+r)!}{n!} \left( 1 + \frac{n}{n+r} \right) = (-)^t \frac{(t+r)!}{t!} \dots \quad (9a)$$

Substituting (9a) in (9) yields

$$R(y) = y^r \dots \dots \dots \dots \dots \dots \quad (10)$$

This completes the proof for the elementary downwash  $w_r$ . Obviously this proof also covers any arbitrary downwash distribution  $w(x)$  which can be obtained by linear superposition of elementary distributions  $w_r$ .

3.5.3. *Part solution for  $M = 1 - \delta$ .*—The asymptotic expression 3.5.1(3) for the Poissio kernel  $k(\mathbf{x})$  suggests the approximation

$$k(\mathbf{x}) \simeq k_0(\mathbf{x}) = \begin{cases} K \left( \frac{2\mathbf{x}}{1+M} \right) \exp \left( i \frac{1-M}{1+M} \mathbf{x} \right) & \text{if } \mathbf{x} > 0 \\ 0 & \text{if } \mathbf{x} < 0 \end{cases} \dots \dots \quad (11)$$

The ‘modified kernel’  $k_0(\mathbf{x})$  is integrable whereas  $k(\mathbf{x})$  is not ; of course the approximation (11) is valid only if  $v/\mathbf{x}$  is sufficiently large (*see* Table 6 and Fig. 7).

The function  $k_0(\mathbf{x})$  has some analytical interest in that the solution of the ‘modified Poissio equation’—3.5(1) with  $k_0(\mathbf{x})$  instead of  $k(\mathbf{x})$ —can readily be derived, *see* Appendix IV. In particular the gradient of the modified forces at the point  $M = 1$  can be given, *see* AIV(6). It appears that the amount of this gradient is about one quarter of the amount of the forces themselves—compare 3.4.1(4). Unfortunately this gradient of the modified solution is not identical with the gradient of the correct solution—this can be seen from 3.5.1(3)—and the modified solution itself can be considered a useful approximation only if  $\nu$  is rather large—this can be seen from 3.5(1) and Fig. 7.

---

†Some care has to be taken in the case  $r = 0$  which is to be understood as the limit  $r \rightarrow 0$ . Thus

$$\left( \frac{2n+r}{n+r} \right)_{\substack{n=0 \\ r=0}} = \lim_{r \rightarrow 0} \left( \frac{0+r}{0+r} \right) = 1 \dots \dots \dots \dots \quad (7a)$$

3.5.4. *Remark on complete solution.*—In Figs. 1e and 1f curves of the subsonic and supersonic lift coefficients are shown side by side. The curves for  $M = 0.8, 0.9, 0.95$  are interpolations, see section 4.1; the remaining curves represent the correction solution.

To the curves  $M = 0.8, 0.9, 0.95$  correspond the curves  $M = 1.25, 1.11, 1.05$ . The latter are of a trochoidal nature; interpolation between  $M = 1$  and  $M = 1.43$  would lead to considerable error. However this does not necessarily reflect on the reliability of interpolation in the range  $0.7 < M < 1$ : a comparison of the two corresponding curves  $M = 1.43$  and  $0.7$  with the curve  $M = 1$  would suggest, on the contrary, that though interpolation is of little value for  $M = 1 + \delta$  it will yield reasonable approximations for  $M = 1 - \delta$ . This will now be supported by a discussion of the different natures of the lift distributions  $p(x)$  in the two regions  $M = 1 \pm \delta$ .

The trochoidal nature of the curves  $M = 1 + \delta$  arises from the waviness of the lift function  $p(x)$  (see Fig. 2†). This waviness in its turn corresponds to the short-waved part of the perturbation field AII(3) and originates, in the first instance, in the disturbance formed by the leading edge; its amplitude decreases as the impulse travels on. A similar short-waved perturbation will occur in subsonic flow, see AII(1)‡, but in this case the impulse travels forward, originating at the trailing edge. The difference in question between the supersonic and the subsonic lift distributions must therefore be due to a difference between the boundary conditions for the leading edge,  $M \geq 1$ , and the trailing edge,  $M \leq 1$ .

We may put our problem as follows: for  $M = 0$  a rapidly convergent (and often used) representation of  $p(x)$  is

$$p(x) = \sqrt{\left\{\frac{1-x}{x}\right\}} \sum_0^{\infty} c_{0n} x^n \quad (M = 0). \quad \dots \dots \dots (12)$$

For  $M = 1$  from 3.4.2(11)

$$p(x) = \frac{C}{\sqrt{x}} \sum_0^{\infty} c_{1n} x^n \quad (M = 1) \quad \dots \dots \dots (12a)$$

is again rapidly convergent. Thus for  $M \leq 1$  we may write tentatively

$$p(x) = \frac{G(x, M)}{\sqrt{x}} \sum_0^{\infty} c_{Mn} x^n \quad (M \leq 1). \quad \dots \dots \dots (13)$$

For the convergency of (13) to be uniform in  $M$  we must impose the condition that the function  $G(x, M)$  exhibits the waviness of the form  $\exp\{2iM\hat{x}/(1-M)\}$ , discussed above, and also that

$$G(x, M) \rightarrow \begin{cases} \sqrt{1-x} & (M \rightarrow 0) \\ C & (M \rightarrow 1) \end{cases} \quad \dots \dots \dots (13a)$$

The further condition

$$G(x, M) \doteq \text{const} \sqrt{\left\{\frac{1-x}{x}\right\}} \quad \begin{matrix} (x \doteq 1) \\ (M \doteq 1) \end{matrix} \quad \dots \dots \dots (13b)$$

arrived at as follows:

† See in particular  $p_2'$ ,  $M = 1.111$ . Note that the position of the trailing edge is given by  $\hat{x} = 2/\nu$ .

‡ Strictly not the field of a single source as discussed in AII but the field of a line of doublets should be considered. This latter field is represented, in its essence, by  $k(\nu x) = k(2\hat{x})$ , see 3.5(3), and shows the same two types of wave perturbations.

Writing for the lift distributions  $p(x)$  belonging to a given downwash  $w(x)$  but various Mach numbers  $M \leq 1$

$$p(x) \sim \begin{cases} x^\alpha & \text{near leading edge } (x \approx 0) \\ (1-x)^\beta & \text{near trailing edge } (x \approx 1) \end{cases} \quad \dots \dots \dots \quad (14)$$

we know

$M$	0	1				
$\alpha$	-0.5	-0.5	..	..	..	(14a)
$\beta$	+0.5	0				

Thus we expect  $\alpha$  to equal  $-0.5$ , as is implied in (13), for all  $M$  not exceeding unity. As regards  $\beta$ , we might suspect that  $\beta$  tends to zero as  $M$  tends to unity for  $\nu$  not zero. That this is not possible appears from the integral AI(6) which occurs for 3.5(1) owing to 3.5(1a). Obviously the term with  $x^\alpha$  in AI(6) must disappear in order that 3.5(1) can be satisfied; the same applies to a corresponding term  $(1-x)^\beta$  which arises from the symmetry of 3.5(1). Thus

$$\alpha, \beta = 0.5 \pmod{1} \quad (M < 1) \quad \dots \dots \dots \quad (14b)$$

in confirmation of (13). (13b) then follows.

The above set of conditions for the function  $G(x, M)$  appears to be rather stringent and the fact that it is fulfilled by a fairly simple function makes it likely that this function would be a suitable choice in our tentative series (13). This function is

$$G(x, M) = \sqrt{\left\{ \frac{\pi(1+M)}{2M} \right\}} F\left(\frac{M\nu(1-x)}{1-M}\right) \quad \dots \dots \dots \quad (15)$$

It is plotted in Fig. 8; we have, compare AI(2)

$$G(x, 0) = \sqrt{\nu(1-x)}; \quad G(x, 1) = \frac{1}{2}(1-i)\sqrt{\pi} \quad \dots \dots \dots \quad (15a)$$

It is significant that  $G(x, M)$  is again a Fresnel integral and thus is nearly related to the solution for  $M = 1$ .

Figs. 2 and 8 show the different natures of the lift distributions  $p(x)$  in the two regions  $M = 1 \pm \delta$ . As  $M$  tends to unity from the supersonic side (Fig. 2) the waves formed by  $p(x)$  contract to the left and pass the trailing edge (which is determined by  $\hat{x} = \frac{1}{2}\nu$ ) thus giving rise to the oscillating term  $\exp(-\nu)$  in the force coefficients, see 3.3(2), (6). A similar process occurs as  $M$  tends to unity from the subsonic side (Fig. 8) though in the opposite direction. The essential difference however is that as  $M$  tends to unity the amplitude of the waves remains nearly unchanged at a given point  $\hat{x}$  of Fig. 2 but tends to zero at a given point  $x < 1$  of Fig. 8. This difference explains why interpolation may be used for  $M = 1 - \delta$  but not for  $M = 1 + \delta$ . Clearly the change in the wing force coefficients (*i.e.*, of the integrals of  $p(x)$ ) has a higher order of smoothness when  $M$  tends to unity from the subsonic side than when  $M$  tends to unity from the supersonic side†.

The cause of the difference just discussed is indeed the difference in the boundary conditions at the leading and trailing edges; the limit function is of order  $1/\sqrt{x}$  in Fig. 2, constant in Fig. 8. Thus the maximum amplitude of the waves must increase indefinitely as  $M$  tends to unity in Fig. 2 but remains constant (roughly) in Fig. 8.

---

†It also follows that the limit  $M = 1 - 0$  of  $p(x)$  exists (while the limit  $M = 1 + 0$  exists only for the mean 3.4.2(12).)

So much for the nature of  $p(x)$ . An actual numerical computation on the basis of (13) and (15), even if simplified by means of sections 3.5.1 and 3.5.3, would still require a considerable amount of work. This work does not appear to be justified in view of

(a) the relatively small degree of physical validity which can be expected for the correct linear solution,

(b) the conclusion (which can be drawn from the above argument) that interpolation through the range  $M = 1 - \delta$  will lead to a reasonable approximation to the linear solution.

3.5.5. *Discussion of existing numerical results for  $M \leq 0.8$ .*—As may be seen from Fig. 8, the waviness of the lift function  $p(x)$  does not become pronounced in the truly subsonic range,  $M \leq 0.8$ , say, at least not for moderate frequencies ( $\nu \leq 1.5$ , say). A number of numerical solutions for this range have been published, notably by Frazer and Skan<sup>19</sup> [ $M \leq 0.7$ ], Dietze, Turner and Rabinowitz<sup>17</sup> [ $M \leq 0.7$ ], Schade<sup>20</sup> [ $M \leq 0.8$ ] and recently by Timman, van de Vooren and Greidanus<sup>21</sup> [ $M \leq 0.8$ ]. The results of the first three investigations agree with each other satisfactorily but they differ systematically from those of the fourth. The differences are large enough† to warrant a discussion.

Timman<sup>21</sup> starts directly from the linear differential equation while the first three papers use its equivalent integral form, *viz.*, the Possio equation, 3.5(1). However the Possio equation can be taken to be well confirmed‡, so that the difference in the results cannot be explained by this difference in method.

The methods of Frazer<sup>19</sup> and Schade<sup>20</sup> are approximate methods in that in them a number  $N$  of terms to be considered in the series corresponding to 3.5.4(12) has to be chosen initially. The methods of Dietze<sup>17</sup> and Timman<sup>21</sup> are 'exact' methods§ in that in them the summation can be continued until a chosen accuracy is reached.

Schade<sup>20</sup> uses the series

$$p(x) = b \sqrt{\left\{ \frac{1-x}{x} \right\}} + \sum_0^N b_n x^n; \quad p(1) = 0 \quad \dots \dots \dots (17)$$

instead of 3.5.4(12). (17) contradicts 3.5.4(13a) but this should not have an appreciable effect if  $M \leq 0.7$  (see Fig. 8; a confirmation is (16)).

Our further discussion is confined to the two exact methods. These are not very different as far as the representation of the lift distribution  $p(x)$  is concerned. Dietze<sup>17</sup> uses the Fourier series

$$p(x) = a_0 \cot \frac{1}{2}\theta + \sum_1^{\infty} a_n \sin n\theta \quad \dots \dots \dots (18)$$

( $\theta = \cos^{-1}(1 - 2x)$ )

which can be rearranged in the form 3.5.4 (12). Timman *et al.*<sup>21</sup> write

$$p(x) = \bar{p}(x) \exp \left( i \frac{M^2}{1 - M^2} x\nu \right) \quad \dots \dots \dots (19)$$

† An example in point is

$$l'_{z(M=0.7, \nu=1)} = \begin{cases} 0.168 & \text{Refs. 17, 19, 20} \\ 0.244 & \text{Ref. 21} \end{cases} \quad \dots \dots \dots (16)$$

See also Fig. 9.

‡ Section 3.5.2 above may be taken as another confirmation of the Possio equation.

§ Dietze<sup>17</sup>, it is true, uses an approximation of the Possio kernel; however, this approximation should be exact within the accuracy of Dietze's numerical calculation.

and

$$\bar{p}(x) = a_0 \cot \frac{1}{2}\theta + \sum_1^{\infty} b_n s e_n(\pi - \theta) \quad \dots \quad \dots \quad \dots \quad \dots \quad \dots \quad (19a)$$

The  $s e_n$  are Mathieu functions. As

$$s e_n(x) = \sum_1^{\infty} B_m \sin r x \quad \dots \quad \dots \quad \dots \quad \dots \quad \dots \quad \dots \quad \dots \quad (19b)$$

it follows that, by rearrangement of (19a), the function  $\bar{p}(x)$  can also be given the form (18).

The two methods further agree in that the coefficients  $a_n, b_n$  are defined as sums

$$a_n = \sum_0^{\infty} a_{rn}; \quad b_n = \sum_0^{\infty} b_{rn}$$

and that successive terms  $a_{rn}, b_{rn}$  are obtained from recurrence relations.

The essential difference between the two methods would thus seem to be the exponential factor in (19). This factor has the following significance:

The perturbation field AII(1) of a moving source exhibits the two wavelengths

$$w_1 = \frac{2\pi c}{vM} (1 + M); \quad w_2 = \frac{2\pi c}{vM} (1 - M) \quad \dots \quad \dots \quad \dots \quad \dots \quad \dots \quad (20)$$

However, writing for the velocity potential  $\bar{\varphi}$ , in accordance with (19),

$$\bar{\varphi} = \bar{\varphi} \exp\left(i \frac{M^2}{1 - M^2} v x\right) \quad \dots \quad \dots \quad \dots \quad \dots \quad \dots \quad (20a)$$

we find

$$\bar{\varphi} = \frac{-Q}{4\pi |x|} \exp\left(-i \frac{Mv}{1 - M^2} |x|\right) \quad \dots \quad \dots \quad \dots \quad \dots \quad \dots \quad (20b)$$

with only one wavelength

$$w_3 = \frac{2\pi c}{vM} (1 - M^2) \quad \dots \quad \dots \quad \dots \quad \dots \quad \dots \quad \dots \quad \dots \quad (20c)$$

Thus  $\bar{\varphi}$ , and therefore  $\bar{p}$ , correspond to a medium at rest.

For the speed range  $M = 1 - \delta$ , neither method appears to be suitable. In both methods the respective solutions ( $p(x), \bar{p}(x)$ ) exhibit waves the length of which ( $w_2, w_3$ ) tends to zero as  $M$  tends to unity; the respective series (18), (19a) become progressively more unsuitable for representing these waves. The  $n$ th term of (18) has  $n$  nodes along the chord while the  $n$ th term of (19a) has only  $\frac{1}{2}n$  nodes; as against this,  $w_3$  tends to  $2w_2$  as  $M$  tends to unity. Thus neither method appears to have an advantage over the other in this respect.

We now return to the differences, mentioned at the beginning of this section, between the two sets of numerical results. An independent repetition of Timman's work would be rather laborious as the analysis and numerical work are both rather involved. On the other hand Dietze's analysis has been thoroughly checked by Turner and Rabinowitz<sup>17</sup>, who have also repeated his numerical calculation. A possible objection to Dietze's method is that its convergency has not been proved generally; however for  $M = 0.7, v = 1$ , *i.e.*, for the case of equation (16), this convergency has now been re-checked carefully and was found to be of order  $2^{-n}$  at least.

In view of this position, and as Dietze's results agree well enough with the results by Frazer<sup>19</sup> and Schade<sup>20</sup>, the results<sup>17</sup> obtained by Dietze's method have been preferred to Timman's results<sup>21</sup> as a basis for the main tables of the present report.†

3.6. *Survey of the Solutions.*—In Fig. 2 the lift distributions  $p(x)$  due to vertical translation and to pitch are plotted for different Mach numbers  $M \geq 1$  (and also for  $M = 0$ ). The position of the trailing edge is given by  $\hat{x} \equiv \nu x/2 = \nu/2$ . The true local lift  $p(x)$  has no limit as  $M$  tends to unity, but the mean local lift

$$p_m(x) = \lim_{\varepsilon \rightarrow 0} \frac{1}{2\varepsilon} \int_{x-\varepsilon}^{x+\varepsilon} p(\xi) d\xi \quad \dots \quad \dots \quad \dots \quad \dots \quad \dots \quad \dots \quad \dots \quad (1)$$

has a limit. The nature of the subsonic lift distributions  $p(x)$  is indicated by a function  $G$ , Fig. 8. Here the limit  $M \rightarrow 1$  exists without proviso.

The solution for  $M = 1$  is the common limit of both the supersonic solution and the subsonic solution. It has a particularly simple analytical form 3.4.2(11). This simplicity is illustrated graphically in Fig. 5, where the response function  $P$  defined by

$$p(x) = \frac{1-i}{\sqrt{\nu x}} P(x) w(x) \quad \dots \quad \dots \quad \dots \quad \dots \quad \dots \quad \dots \quad \dots \quad (2)$$

is shown for different downwash distributions  $w(x) = x_r$ .

The four main wing force coefficients for  $M = 1$  are given by 3.4.1(2). They are series of powers ( $n - 0.5$ ) of  $\nu$ , while the corresponding supersonic series are series of the integral powers of  $\nu$ . Corresponding relations 3.4.1(2b), (3a) respectively, are valid for the two types of series. The aerodynamic coefficients of the wing with aileron and tab are implicitly given by these four main coefficients.

In addition, asymptotic expressions for the force coefficients are given for  $M = 1 + \delta$ , see 3.3(1), (2), (6). These expressions are useful when  $\nu/\sqrt{M^2 - 1}$  is large ( $> 3$ , say). For  $M = 1 - \delta$  the asymptotic expression for the Possio kernel is given 3.5.1(3), and also the solution for the main part of the kernel, Appendix IV. In section 3.5.4 it is shown that interpolation (which is of little value for  $M = 1 + \delta$ ) will yield reasonable results for  $M = 1 - \delta$ .

In section 3.5.5 it is explained why the numerical results of Dietze<sup>17</sup> are thought to be reliable in spite of differing results recently published.

4. *Tables and Graphs of Wing Force Coefficients.*—The four main wing force coefficients‡ are tabulated in Table 2 ( $\nu \leq 1.4$ ) and are shown in isometric presentation in Figs. 1a to 1d ( $\nu \leq 1$ ). Additional values for  $M = 1$  and  $M = 1.05$  are given in Table 3.

The following sources were used in the different speed ranges (for  $M = 0.8, 0.9, 0.95$  see section 4.1):

- (a)  $M = 0$ : Standard results
- (b)  $M = 0.5, 0.6, 0.7$ : Turner and Rabinowitz<sup>17</sup>, tables for  $\nu = 0(0.04) 0.2(0.2) 1.4$
- (c)  $M = 1$ : Equations 3.4.1(2), (2a), (2b)
- (d)  $M = 1.05, \nu \leq 0.35$ : Additional tables calculated by D. L. Woodcock, printed in Temple and Jahn<sup>7</sup>. Parameter of this table is  $y = \nu M^2/(M^2 - 1)$

† After this report was written (early in 1952) several notes on the subject have been published; see Jordan<sup>22</sup>.

‡ For definitions see section 3.2 and Table 1.

§ An error in this table was discovered when the asymptotic formula section 3.3 was checked. The corrected values are given in Table 5.

(e)  $M = 1.05$ ,  $\nu \geq 0.4$ : Equations 3.3(1), (2), (6)

(f)  $M \geq 1.111$ : Jordan<sup>13</sup>, tables for  $\dagger \log_{10}(\nu/2) = -2(0.05)0$ .

Accuracy: The present tables should be accurate (*i.e.*, should give the correct solution of the linear problem) to less than a unit in the last decimal place in cases (a), (c) and (e). In the remaining cases errors arise from the following reasons:

- (i) Inaccuracy of source: for case (b), the results of Turner and Rabinowitz<sup>17</sup> should be accurate to within 1 per cent $\ddagger$ , and should usually be better.
- (ii) In cases (b) and (f) the factor  $\pi$  or  $\frac{1}{2}\pi$  in the transformation (Table 1) introduces an error in the fourth decimal place of  $l_z$ ,  $l_a$  and  $m_z$  — up to 2 units for  $l_z$  (factor  $\pi$ ) and up to 1 unit for  $l_a$  and  $m_z$  (factor  $\frac{1}{2}\pi$ ). $\S$
- (iii) In case (d) there is an error in the imaginary part of each derivative of up to 3 units in the fourth decimal place, due to the factor  $\nu$  in the transformation.
- (iv) Interpolation: Some of the values given for case (b) and all of the values for cases (d) and (f) had to be obtained by interpolation with respect to  $\nu$ . Third-order interpolation was used throughout. Last decimal figures (usually the fourth only, but exceptionally the third as well) have been omitted in those regions where the estimated maximum error due to interpolation exceeded 3 units of the cancelled decimal place.

4.1. Range  $0.7 < M < 1$ .—It is not claimed that the table entries for  $M = 0.8, 0.9$  and  $0.95$  (Table 2) represent the correct solution with the same degree of accuracy as do the other entries of the same tables; they are nothing but the formal result of what seemed to be the most reasonable method of interpolation based on these other entries.

Different interpolations are shown in Fig. 9 for the case  $\nu = 0.8$ , *viz.*, the interpolations based on the table entries for  $M = 0.5$  (not (A)),  $M = 0.6, 0.7$  and  $1.0$ :

- (A) Second order in  $M$
- (B) Third order in  $M$
- (C) Third order in  $\nu = 1 - M^2$ .

From 3.5.1(3) it appears that (C) is preferable if  $\nu$  is sufficiently large; hence (C) is entered in Table 2 and is shown in Figs. 1e and 1f. The isometric graphs Figs. 1a to 1d, show the interpolation (A) (the difference is usually hardly visible owing to the small scale of the graphs).

In addition to the interpolations (A) to (C), Fig. 9 also shows values obtained from other sources:

$$\left. \begin{array}{l} \text{Schade}^{20}, \text{ tables for } \nu = 0(0.4)2 \\ \text{Timman } et \text{ al.}^{21}, \text{ tables for the parameter } \nu M/(1 - M^2) \end{array} \right\} M \leq 0.8.$$

Of these, the values for  $M = 0.8$  (interpolated for frequency parameter in the case of Ref. 21) are tabulated in Table 4.

$\dagger$  Constant steps  $\Delta \log \nu$  are more logical than constant steps  $\Delta \nu$ . The first arrangement is preferable if a value of the parameter  $\nu$  is chosen for the individual flutter calculation; however it is somewhat inconvenient in those cases where  $\nu$  is the unknown quantity.

$\ddagger$  With possible exceptions near the corner  $M = 0.7, \nu = 1.4$  of the region covered.

$\S$  This does not apply in case (b) to table entries less than  $\pi/10$  for  $l_z$ , or less than  $\pi/20$  for  $l_a$  and  $m_z$ .

The reason why Ref. 21 has not been made use of in the main Table 2 has been stated in section 3.5.5. Schade's values have been excluded for two reasons :

- (a) They are so few that interpolation with regard to  $\nu$  becomes doubtful
- (b) Interpolation with regard to  $M$  becomes less straightforward if Schade's values are included ; see, e.g.,  $l_a''$  and  $m_a'$  in Figs. 9c and 9d.

Discussing (b), we must distinguish :

- (i) The curves which represent the correct linear solution. These curves are waved ; wavelengths and amplitudes decrease as  $M$  tends to unity.
- (ii) Curves which approximate (i) reasonably well but smooth out the waviness of (i). The aim of our interpolation are curves (ii). The observation (b) may have one or both of two reasons :
  - (I) The curves (ii) are appreciably more strongly curved than is anticipated in our interpolation formula
  - (II) The difference between (i) and (ii)—which we assumed to be negligible for  $M \leq 0.7$ —is already appreciable for  $M = 0.8$  (Schade's values lie on (i)).

It is difficult to decide which of the two reasons is correct or preponderates. For our aim, a good average of approximation, it seemed safer to choose the simpler curves, *i.e.*, to exclude Schade's values.

Lastly the significance for the present interpolation of recently published solutions† of the subsonic problem for the range  $\nu M/\sqrt{M^2 - 1} \gg 1$  needs to be discussed. Of these solutions the one by W. P. Jones<sup>23</sup> is the best, giving good approximation up to  $\nu \approx 0.2$  for  $M = 0.7$ . However, to  $\nu = 0.2$  for  $M = 0.7$  corresponds in accuracy  $\nu \approx 0.15$  for  $M = 0.8$ ,  $\nu \approx 0.10$  for  $M = 0.9$  ; thus even Jones's results are valid only for a small corner of the region covered by our interpolation.

4.2. *Discussion.*—The numerical values given in Table 2 should cover the practical requirements of wing flutter calculations. Interpolation, required in the case of control surface flutter, is convenient for  $M \leq 1$ . Interpolation with respect to both  $M$  and  $\nu$  is difficult in a certain range  $M = 1 + \delta$  because of the short waves which characterise the curves in this range. However these waves can be expected to have little physical significance (*see* section 2.1) ; the force coefficients for this range can be replaced by coefficients for  $M = 1$ .

Little need be said about the isometric graphs of Fig. 1, except perhaps that the often discussed region of negative damping in pitch (*see* Fig. 3) corresponds to the funnel  $-m_a'' < 0$  in Fig. 1d. The graphical representation has been truncated at the plane  $-m_a'' = -1.4$  ; the coefficient  $m_a''$  itself reaches arbitrarily large values near the point  $[M, \nu] = [1, 0]$ . When three-dimensional effects are allowed for, the  $\nu, M$ —region of negative damping is reduced but it persists‡ in a region near the point  $[M, \nu] = [1, 0]$ —as indeed would be expected from Fig. 1d.

5. *Conclusion.*—Linear theory is applicable to the two-dimensional problem of the oscillating wing of zero thickness, even at sonic speed. In order to facilitate such application the four main wing coefficients have been tabulated (and illustrated by isometric graphs) in the speed range  $0 \leq M \leq 2$ . Further, the complete solution for an arbitrary downwash at sonic speed has been given in a form convenient for numerical evaluation. For near-sonic speeds, this sonic solution is preferable, as an approximation to the non-linear solution, to the 'exact' linear solution.

† By Miles<sup>22</sup>, W. P. Jones<sup>23</sup>, Radok<sup>24</sup>, Neumark<sup>25</sup>.

‡ *See, e.g.*, Runyan, Cunningham and Watkins<sup>26</sup>.



## REFERENCES

- | <i>No.</i> | <i>Author</i>                               | <i>Title, etc.</i>   |
|------------|---|--|
| 1          | C. C. Lien, E. Reissner and H. T. Tsien     | On two-dimensional non-steady motion of a slender body in compressible fluid. <i>J. Math. Phys.</i> Vol. XXVII, p. 220. 1948.  |
| 2          | P. F. Jordan .. .. .                        | Flutter at subsonic and supersonic speeds. A.R.C. 9813. 1946. (Unpublished.)   |
| 3          | M. A. Heaslet, H. Lomax and J. R. Spreiter  | Linearised compressible-flow theory for sonic flight speeds. N.A.C.A. Report 956. 1950.  |
| 4          | N. Rott .. .. .                             | Oscillating airfoils at Mach number 1. <i>J. Ae. Sci.</i> Vol. 16, p. 380. 1949.   |
| 5          | N. Rott .. .. .                             | Flügelschwingungsformen in ebener kompressibler Potentialströmung <i>Z.A.M.P.</i> Vol. I, p. 380. 1950.  |
| 6          | H. C. Nelson and J. H. Berman ..            | Calculations on the forces and moments for an oscillating wing-aileron combination in two-dimensional potential flow at sonic speed. N.A.C.A. Report 1128. 1953. (Formerly N.A.C.A. Tech. Note 2590. January, 1952.)   |
| 7          | G. Temple and H. A. Jahn .. ..              | Flutter at supersonic speeds: Derivative coefficients for a thin airfoil at zero incidence. R. & M. 2140. April, 1945.   |
| 8          | I. E. Garrick .. .. .                       | Some research on high-speed flutter. Third Anglo-American Aeronautical Conference. Brighton, 1951.   |
| 9          | W. P. Jones and S. W. Skan .. ..            | Aerodynamic forces on biconvex aerofoils oscillating in a supersonic airstream. R. & M. 2749. August, 1951.  |
| 10         | W. J. Tuovila, J. E. Baker and A. A. Regier | Initial experiments on flutter of unswept cantilever wings at Mach number 1.3. N.A.C.A. Research Memo. L8J11. 1949.  |
| 11         | J. B. Bratt and A. Chinneck .. ..           | Measurements of mid-chord pitching moments at high speeds. R. & M. 2680. June, 1947.   |
| 12         | L. Schwarz .. .. .                          | Ebene instationäre Theorie der Tragfläche bei Überschallgeschwindigkeit. Jahrbuch, 1943. der Deutschen Luftfahrtforschung.   |
| 13         | P. F. Jordan and M. Gawehn .. ..            | Unsteady aerodynamical coefficients for supersonic flow. A.R.C. 10,052 and A.R.C. 11,400. 1946. (Translation from German.)   |
| 14         | L. Schwarz .. .. .                          | Untersuchung einiger mit den Zylinderfunktionen nullter Ordnung verwandter Funktionen. <i>L.F.F.</i> Vol. 20, p. 341. 1943. Reprinted as A.R.C. 8,699.   |
| 15         | E. T. Copson .. .. .                        | <i>Theory of Functions.</i> Oxford University Press. 1935.   |
| 16         | I. T. Minhinnick .. .. .                    | Subsonic aerodynamic flutter derivatives for wings and control surfaces. R.A.E. Report Structures 87. A.R.C. 14,228. 1950: and Addendum, A.R.C. 14,855. 1952.  |
| 17         | F. Dietze .. .. .                           | The air forces for the harmonically oscillating aerofoil in a compressible medium at subsonic speeds (two-dimensional problem). 1943. A.R.C. 10,219. (Translation from German.) This paper has been translated, thoroughly checked, corrected and extended by: |
|            | M. J. Turner and S. Rabinowitz ..           | Chance Vought Aircraft Report GTR-65 (1947). The corrections and extensions are reprinted in N.A.C.A. Tech. Note 2213. October, 1950.  |
| 18         | L. Schwarz .. .. .                          | Zahlentafeln zur Luftkraftberechnung der schwingenden Tragfläche in kompressibler ebener Unterschallströmung. ZWB FB 1838. 1943. These tables have been extended by:   |
|            | Th. Schade .. .. .                          | ZWB UM 321. 1944. A.R.C. 9,506. (See Ref. 20.)   |
| 19         | R. A. Frazer and S. W. Skan .. ..           | Possio's subsonic derivative theory and its application to flexural-torsional wing flutter. R. & M. 2553. 1942.  |

REFERENCES—continued

No.	Author	Title, etc.
20	Th. Schade .. .. .	The numerical solution of Possio's integral equation for an oscillating aerofoil in a two-dimensional subsonic stream (1944/6). A.R.C. 9,506, A.R.C. 10,108 and Addendum. (Translation from German.)
21	R. Timman, A. I. van de Vooren and J. H. Greidanus	Aerodynamic coefficients of an oscillating aerofoil in two-dimensional subsonic flow. <i>J. Ae. Sci.</i> Vol. 18, p. 797. 1951.
22	John W. Miles .. .. .	Quasi-stationary aerofoil theory in compressible flow. <i>J. Ae. Sci.</i> Vol. 16, p. 509. 1949. Also <i>Quart. App. Math.</i> Vol. VII. 1949.
23	W. P. Jones .. .. .	Oscillating wings in compressible subsonic flow. A.R.C. 14,336. 1951.
24	J. R. M. Radok .. .. .	An approximate theory of the oscillating wing in a compressible subsonic flow for low frequencies. N.L.L. Report F.97. September, 1951.
25	S. Neumark .. .. .	Two-dimensional theory of oscillating aerofoils. R.A.E. Report Aero 2449. A.R.C. 14,889. 1952.
26	H. L. Runyan, H. J. Cunningham and Ch. E. Watkins	Theoretical investigation of several types of single-degree-of-freedom flutter. <i>J. Ae. Sci.</i> Vol. 19, No. 2, p. 101. February, 1952.
27	W. Magnus and F. Oberhettinger ..	<i>Formeln und Sätze für die speziellen Funktionen der mathematischen Physik.</i> Springer, Berlin. 1948 (2nd Ed.)
28	E. T. Whittaker and G. N. Watson ..	<i>A Course of Modern Analysis.</i> Cambridge University Press. 1946. (4th Ed.)
29	P. F. Jordan .. .. .	Further comments.....'Reader's Forum'. <i>J. Ae. Sci.</i> Vol. 20, p. 362. 1953.

APPENDIX I

*Basic Mathematical Formula*

(1) Using the notation defined in section 3.1 we obtain† the following asymptotic expressions for Bessel functions of the first kind,  $J_p(x)$ , and Bessel functions of the second kind (Weber's form)  $N_p(x)$  (also called Neumann functions)

$$\left\{ \begin{array}{l} J_p(x) \\ iN_p(x) \end{array} \right\} \sim \frac{i^p}{\pi(2i\pi x)^{0.5}} \sum_0^\infty \frac{\overline{m+p}! \overline{m-p}!}{m!(2ix)^m} [e^{ix} \pm i(-)^{m+p} e^{-ix}]. \quad \dots \quad (1)$$

Thus the Hankel functions (or Bessel functions of the third kind)

$$\left\{ \begin{array}{l} H_p^{(1)}(x) = J_p(x) + iN_p(x) \\ iH_p^{(2)}(x) = iJ_p(x) + N_p(x) \end{array} \right\} \sim \pm 2 \frac{e^{\pm ix}}{\pi(2i\pi x)^{0.5}} \sum_0^\infty (\pm i)^{p-m} \frac{\overline{m+p}! \overline{m-p}!}{m!(2ix)^m}. \quad \dots \quad (1a)$$

If  $x$  is real and positive—in the present report this is always the case—then the amount of the error which is committed by breaking off after the  $n$ -th term is smaller than the amount of the  $(n+1)$ -th term.

† See, e.g., Magnus and Oberhettinger<sup>27</sup> p. 34. Note that

$$\frac{1}{4m} (4p^2 - 1)(4p^2 - 3^2) \dots (4p^2 - (2m-1)^2) = \frac{(-)^{m+p}}{\pi} \overline{m+p}! \overline{m-p}!.$$

(2) The Fresnel integrals  $C(x)$  and  $S(x)$ , see, e.g., Ref. 26, we use in the combination

$$\begin{aligned} F(x) &= C\left(\sqrt{\frac{2x}{\pi}}\right) - iS\left(\sqrt{\frac{2x}{\pi}}\right) = \frac{1}{\sqrt{2\pi}} \int_0^x e^{-iu} \frac{du}{\sqrt{u}} \\ &= \sqrt{\frac{2x}{\pi}} \sum_0^{\infty} \frac{(-ix)^n}{n!(2n+1)} = e^{-ix} \sqrt{\frac{x}{2}} \sum_0^{\infty} \frac{(ix)^n}{n+1!} \quad \dots \quad \dots \quad \dots \quad \dots \end{aligned} \quad (2)$$

(see (4c) below). For large  $x$

$$F(x) = \frac{1-i}{2} + \frac{i}{\sqrt{2\pi x}} e^{-ix} + O\left(\frac{1}{x}\right). \quad \dots \quad \dots \quad \dots \quad \dots \quad (2a)$$

A graphical illustration is Fig. 8 where

$$G(x, M) = \sqrt{\left\{\frac{\pi(1+M)}{2M}\right\}} F\left(\frac{M\nu(1-x)}{1-M}\right)$$

is plotted.

(3) The interesting relation

$$\sum_{m=0}^n \binom{n}{m} (-1)^m \frac{(m+a)!}{(m+a+b)!} = \frac{a!}{(b-1)!} \frac{(n+b-1)!}{(n+a+b)!} \quad \dots \quad \dots \quad (3)$$

can be proved by means of the integral (5); however (3) is more elementary than (5) and hence deserves an independent elementary proof:

Note first that it is sufficient to prove (3) for  $a = 0, 1, 2, \dots, n$  (multiplication by  $(n+a+b)!/a!$  leads to an  $n$ th order expression in  $a$  on the left, while the right-hand side becomes independent of  $a$ ).

Consider the case  $a = 0$ , i.e.,

$$\sum_{m=0}^n (-1)^m \frac{n!}{(n-m)!} \frac{b!}{(m+b)!} = \frac{b}{n+b}. \quad \dots \quad \dots \quad \dots \quad (3a)$$

Assume (3a) to be correct if  $[n, b]$  is replaced by  $[n-1, b+1]$ . The sum in (3a) can be transformed to read

$$1 - \frac{n}{b+1} \sum_0^{n-1} (-1)^m \frac{(n-1)!}{(n-1-m)!} \frac{(b+1)!}{(m+b+1)!} = 1 - \frac{n}{b+1} \frac{b+1}{n+b} = \frac{b}{n+b}.$$

From this and the fact that (3a) is obviously correct for  $n = 0$  or  $1$ , for all values of  $b$ , it follows that (3a) is correct for any number  $n$ .

Now assume that (3) is correct when  $a$  is replaced by  $(a-1)$ ; then

$$\begin{aligned} \sum_{m=0}^n \binom{n}{m} (-1)^m \frac{(m+a)!}{(m+a+b)!} &= \sum_{m=0}^n \binom{n}{m} (-1)^m \frac{(m+a-1)!}{(m+a+b)!} (m+a+b-b) \\ &= \frac{(a-1)!(n+b-1)!}{(b-1)!(n+a+b-1)!} - b \frac{(a-1)!(n+b)!}{b!(n+a+b)!} \\ &= \frac{a!(n+b-1)!}{(b-1)!(n+a+b)!}. \end{aligned}$$

It follows from this, since (3) has been shown to be correct for  $a = 0$ , that (3) is correct for  $a = 1, 2, \dots, n$ , and therefore for all values of  $a$

This completes the proof.

A particular form of (3) is

$$\sum_{m=0}^n \binom{n}{m} (-)^m \bar{m} = \bar{n} \quad \dots \quad \dots \quad \dots \quad \dots \quad \dots \quad \dots \quad \dots \quad (3b)$$

(4) Some infinite series :

$$\frac{1}{\sqrt{\pi}} \sum_{n=0}^{\infty} \bar{n} y^n = \frac{1}{(1-y)^{0.5}} \quad \dots \quad \dots \quad \dots \quad \dots \quad \dots \quad \dots \quad \dots \quad (4a)$$

$$\frac{1}{\pi} \sum_{n=0}^{\infty} \frac{\bar{n}}{n + p + 0.5} = \bar{p} \quad \dots \quad \dots \quad \dots \quad \dots \quad \dots \quad \dots \quad \dots \quad (4b)$$

$$e^y \sum_{n=0}^{\infty} \frac{(-y)^n}{n!} \frac{(n+a)!}{(n+a+b)!} = \sum_0^{\infty} \frac{y^n}{n!} \frac{a!}{(b-1)!} \frac{(n+b-1)!}{(n+a+b)!} \quad \dots \quad \dots \quad (4c)$$

Formula (4a) is well known. (4b) follows from (5a) below, with  $p = n, y = 1$ , by means of (4a) (4c) is equivalent to (3). A special case of (4c) is ( $a = 0; b = -0.5$ ) :

$$e^y \sum_0^{\infty} \frac{(-y)^n}{\bar{n}!} = \frac{1}{\sqrt{\pi}} \sum_0^{\infty} \frac{y^n}{n! (1-2n)} \quad \dots \quad \dots \quad \dots \quad \dots \quad \dots \quad (4d)$$

(5) The Euler integral of the first kind† is

$$\int_0^1 x^p (1-x)^q dx = \frac{p!q!}{(p+q+1)!} \quad (p, q > -1) \quad \dots \quad \dots \quad \dots \quad \dots \quad (5)$$

for real parameters  $p, q$ . We use it in the form

$$\int_0^y \frac{(y-\eta)^p \eta^{q-p}}{[\eta(y-\eta)]^{0.5}} d\eta = \frac{\bar{p}! \overline{q-p}!}{q!} y^q \quad \dots \quad \dots \quad \dots \quad \dots \quad \dots \quad (5a)$$

By means of (5a)

$$\int_0^y (y-\eta)^r e^{-\eta} \eta^{-0.5} d\eta = r! y^{r+0.5} \sum_{n=0}^{\infty} \frac{(-y)^n}{r+n+1!} \bar{n} \quad \dots \quad \dots \quad \dots \quad \dots \quad (5b)$$

(6) The integral

$$* \int_0^1 \frac{\xi^\alpha}{x-\xi} d\xi = \sum_{n=0}^{\infty} \frac{x^n}{n-\alpha} + x^\alpha \pi \cot \pi \alpha \quad \dots \quad \dots \quad \dots \quad \dots \quad (6)$$

$0 \leq x < 1; \alpha > -1$

---

† See, e.g., Whittaker and Watson<sup>28</sup> p. 253.

can be derived as follows : assume first  $x \neq 0$ ,  $\alpha > 0$ . Then

$$\begin{aligned} \int_0^1 \frac{\xi^\alpha}{x - \xi} d\xi &= \lim_{\epsilon \rightarrow 0} \sum_{n=0}^{\infty} \left\{ \int_0^{x-\epsilon} \frac{\xi^{n+\alpha}}{x^{n+1}} d\xi - \int_{x+\epsilon}^1 \frac{x^n}{\xi^{n+1} - \alpha} d\xi \right\} \\ &= \sum_{n=0}^{\infty} \frac{x^n}{n - \alpha} - x^\alpha \sum_{n=-\infty}^{+\infty} \frac{1}{n - \alpha}. \end{aligned}$$

From this (6) follows ; see e.g., Ref. 28, p. 136.

In the limit  $\alpha \rightarrow 0$  from (6) formally

$$\lim_{\alpha \rightarrow 0} \int_0^1 \frac{\xi^\alpha}{x - \xi} d\xi = \lim_{\alpha \rightarrow 0} \left\{ -\frac{1 - x^\alpha}{\alpha} + \sum_{n=1}^{\infty} \frac{x^n}{n} \right\} = \log \frac{x}{1 - x}$$

—the correct result. It is also obvious that (6) remains correct for  $x \rightarrow 0$ . It follows at once from the relation

$$\int \frac{\xi^\alpha}{x - \xi} d\xi = \frac{1}{x} \int \left( \xi^\alpha + \frac{\xi^{\alpha+1}}{x - \xi} \right) d\xi$$

that (6) is also correct for  $0 > \alpha > -1$ .

## APPENDIX II

### *Perturbation Potential of Moving Source*

Consider the perturbation field of a disturbance the speed of which passes through the sonic range. The aim of the Appendix is to record briefly the nature of this field in its simplest form.

The perturbation potential  $\varphi = \bar{\varphi} \exp(2i\pi ft)$  of a single oscillating source  $S$  of intensity  $Q \exp(2i\pi ft)$ , acting at the origin of the moving co-ordinates, is given on the  $x$ -axis and for  $M < 1$  by

$$\bar{\varphi} = \frac{-Q}{4\omega|\hat{x}|} \exp\left(-\frac{2iM|\hat{x}|}{1 \pm M}\right) \quad \begin{matrix} (x \gtrless 0) \\ (M < 1) \end{matrix} \quad \dots \quad \dots \quad \dots \quad \dots \quad (1)$$

where the variable sign is  $+$  or  $-$  according as  $x >$  or  $<$   $0$ , and  $\omega = 2\pi/\nu$ . Thus a long-waved perturbation occurs to the rear ( $x > 0$ ) ; it arises from the rearward impulse of  $S$  travelling at the high relative speed  $(1 + M)V_{\text{sound}}$ . The short-waved perturbation to the front ( $x < 0$ ) arises from the forward impulse travelling with the low relative speed  $(1 - M)V_{\text{sound}}$ . The wavelength  $w_1 \simeq 4\pi c/\nu$  of the first is long compared with the wing chord  $c$  and varies little with  $M$  ; the wavelength  $w_2 \simeq 2\pi(1 - M)c/\nu$  of the second tends to zero as  $M$  tends to unity.

Equation (1) remains valid in its essence if the speed is increased to reach the sonic speed, and beyond. For  $M = 1$  the long-waved term takes the simple form

$$\bar{\varphi} = \frac{-Q}{4\omega\hat{x}} \exp(-i\hat{x}) \quad \begin{matrix} (x > 0) \\ (M = 1) \end{matrix} \quad \dots \quad \dots \quad \dots \quad \dots \quad (2)$$

The short-waved term takes the form of the function  $T(y)$  (see 3.4.2(8a)). We may either repeat the argument of 3.4.2(12) or argue that, as the forward speed of the impulse is zero, no point  $x < 0$  will ever be reached by it. By either argument

$$\bar{\varphi} = 0 \quad \begin{matrix} (x < 0) \\ (M = 1) \end{matrix} \quad \dots \quad \dots \quad \dots \quad \dots \quad \dots \quad \dots \quad \dots \quad (2a)$$

At supersonic speed  $(1 - M)V_{\text{sound}}$  is negative; thus the short-waved impulse also travels in the direction of the positive  $x$ -axis:

$$\phi = \begin{cases} \frac{-Q}{4w\hat{x}} \left[ \exp\left(-\frac{2iM\hat{x}}{M+1}\right) - \exp\left(-\frac{2iM\hat{x}}{M-1}\right) \right] & (x > 0) \\ 0 & (x < 0) \end{cases} \quad (M > 1) \quad \dots \quad (3)$$

### APPENDIX III

#### *Possio Kernel ; Asymptotic Formula*

The Possio kernel, see, e.g., Dietze<sup>17</sup>, is

$$\left. \begin{aligned} k(\mathbf{x}) &\equiv k_1(\mathbf{x}) - k_2(\mathbf{x}) \\ k_1(\mathbf{x}) &= \frac{1}{4\sqrt{\kappa}} \left[ H_0^{(2)}\left(\frac{M|\mathbf{x}|}{\kappa}\right) - iM \frac{\mathbf{x}}{|\mathbf{x}|} H_1^{(2)}\left(\frac{M|\mathbf{x}|}{\kappa}\right) \right] \exp(iM^2\mathbf{x}/\kappa) \\ k_2(\mathbf{x}) &= \frac{i}{2\pi} \left[ \log \frac{1 + \sqrt{\kappa}}{M} + \frac{\pi\sqrt{\kappa}}{2} \int_0^{|\mathbf{x}|/\kappa} e^{-i\xi} H_0^{(2)}(M|\xi|) d\xi \right] e^{-i\mathbf{x}} \end{aligned} \right\} \quad (1)$$

$H_p^{(2)}$  are Hankel functions, or Bessel functions of the third kind.

The nature of  $k(\mathbf{x})$  is different in the two ranges  $\mathbf{x} > 0$  and  $\mathbf{x} < 0$ ; see Fig. 6. From now on we assume

$$\mathbf{x} > 0$$

and treat the two cases  $k(\mathbf{x})$  and  $k(-\mathbf{x})$  separately.

Note first that the integral

$$\int_0^\infty e^{\pm i\xi} H_0^{(2)}(M\xi) d\xi = \frac{1}{\sqrt{\kappa}} \left[ i \pm i \pm \frac{2}{\pi} \log \frac{1 - \sqrt{\kappa}}{M} \right] \quad \dots \quad \dots \quad (2)$$

owing to Ref. 12, equations (42), (43).

We use the modified co-ordinates

$$X = \frac{M\mathbf{x}}{\kappa} (\rightarrow \infty); \quad \mathbf{z} = \frac{i}{2X} (\rightarrow 0) \text{ as } M \rightarrow 1. \quad \dots \quad \dots \quad \dots \quad \dots \quad (3)$$

From (1), (2), (3)

$$k_1(\pm \mathbf{x}) = \frac{1}{4\sqrt{\kappa}} \left[ H_0^{(2)}(X) \mp iMH_1^{(2)}(X) \right] e^{\pm iM\mathbf{x}}$$

$$k_2(\pm \mathbf{x}) = \frac{i}{4} \left[ i \pm i \mp \frac{\mathbf{x}}{\sqrt{\kappa}} \int_1^\infty \exp\left(\pm i \frac{X}{M} \eta\right) H_0^{(2)}(X\eta) d\eta \right] e^{\mp i\mathbf{x}} \quad \dots \quad (4)$$

For  $p = 0, 1$  from AI(1a)

$$H_p^{(2)}(X) \sim \frac{1}{\pi} \left( \frac{2i}{\pi X} \right)^{0.5} e^{-i\mathbf{x}} \sum_0^\infty \left( \frac{i}{2X} \right)^m \bar{m} \bar{m}! c_{pm}$$

$$c_{0m} \equiv 1; c_{1m} = -i \frac{2m+1}{2m-1} \quad \dots \quad (5)$$

Thus

$$k_1(\pm \mathbf{x}) \sim \frac{1}{2\pi} \left( \frac{i}{2\pi M \mathbf{x}} \right)^{0.5} \exp\left(-\frac{iM\mathbf{x}}{1 \pm M}\right) \sum_0^\infty \bar{m} \bar{m}! \mathbf{x}^m \left(1 \mp M \frac{2m+1}{2m-1}\right) \quad (6)$$

The integral in  $k_2$  is of the same form as the integral in 3.3(1c). With 3.3(3a) but, instead of 3.2(2a)

$$\left. \begin{aligned} u &= -\frac{i\mathbf{x}}{1+M} \rightarrow -\frac{i\mathbf{x}}{2} \\ v &= \frac{i\mathbf{x}}{1-M} \rightarrow i\infty \end{aligned} \right\} \text{if } M \rightarrow 1 \quad \dots \quad (7)$$

we have

$$A^\pm \equiv \frac{x}{\sqrt{\kappa}} \int_1^\infty \exp(i \pm X\eta/M) H_0^{(2)}(X\eta) d\eta \sim \frac{1}{\pi} \left( \frac{2i\mathbf{x}}{\pi M} \right)^{0.5} \sum_0^\infty \bar{m} \mathbf{x}^m I_m(\alpha) \quad \dots \quad (8)$$

where  $I_m(\alpha)$  is defined by 3.3(3a), and  $\alpha = u, v$ , for  $A^+, A^-$  respectively.

Making use of 3.2(4a), we obtain first

$$A^+ \sim \frac{1}{\pi} \left( \frac{2i\mathbf{x}}{\pi M} \right)^{0.5} \sum_0^\infty \bar{m} \left( \frac{M-1}{2M} \right)^m \left[ I_0(u) + e^{-u} \sum_1^\infty \frac{\overline{n-1!}}{(-u)^n} \right]$$

and then, introducing 3.3(5a), (5) and changing the order of summation we obtain

$$k_2(\mathbf{x}) \sim i \left( \frac{i\mathbf{x}}{\pi(1+M)} \right)^{0.5} e^{-i\mathbf{x}} \sum_0^\infty \left( \frac{i\mathbf{x}}{1+M} \right)^n \frac{1}{n!(2n+1)}$$

$$- \frac{1+M}{2\pi} \left( \frac{i}{2\pi M} \right)^{0.5} \exp\left(-\frac{iM\mathbf{x}}{1+M}\right) \sum_{n=0}^\infty \bar{n}! \mathbf{x}^n \sum_{m=1}^\infty \overline{m+n} \left( \frac{M-1}{2M} \right)^m \quad (9)$$

Also making use of 3.3(4b) we obtain

$$A^- \sim -\frac{1}{\pi} \left( \frac{2i\mathbf{x}}{\pi M} \right)^{0.5} e^{-v} \sum_0^\infty \bar{m} \left( \frac{1+M}{2M} \right)^m \sum_{m+1}^\infty \frac{\overline{n-1!}}{(-v)^n}$$

and

$$k_2(-\mathbf{x}) \sim \frac{1-M}{2\pi} \left( \frac{i}{2\pi\mathbf{x}M} \right)^{0.5} \exp\left(-\frac{iM\mathbf{x}}{1-M}\right) \sum_{n=0}^{\infty} \bar{n}! \mathbf{z}^n \sum_{m=0}^n \frac{1}{n-m} \left( \frac{2M}{1+M} \right)^m. \quad (10)$$

Equations (6), (9), (10) provide the complete asymptotic expression for the Possio kernel  $k = k_1 - k_2$ . It remains to write this set of formulae in a more convenient form.

Consider first the case  $M \rightarrow 1$ . Denote the limit of  $k$  by  $K$ . Thus

$$\begin{aligned} K(\mathbf{x}) &= [k_1(\mathbf{x}) - k_2(\mathbf{x})]_{M \rightarrow 1} \\ &= \left( \frac{i}{2\pi\mathbf{x}} \right)^{0.5} e^{-ix/2} - i \left( \frac{i\mathbf{x}}{2\pi} \right)^{0.5} e^{-ix} \sum_0^{\infty} \left( \frac{i\mathbf{x}}{2} \right)^n \frac{1}{n!(2n+1)} \end{aligned}$$

and finally by means of AI(4d)

$$K(\mathbf{x}) = \left( \frac{i}{2\mathbf{x}} \right)^{0.5} e^{-ix/2} \sum_0^{\infty} - i \left( \frac{i\mathbf{x}}{2} \right)^n \frac{1}{\bar{n}!}. \quad \dots \quad \dots \quad \dots \quad \dots \quad (11a)$$

For negative arguments

$$K(-\mathbf{x}) \equiv 0. \quad \dots \quad \dots \quad \dots \quad \dots \quad \dots \quad \dots \quad \dots \quad \dots \quad (11b)$$

Now return to the general case  $M \leq 1$ . Considering first only the term  $m = 0$  in (6), the first sum in (9), and the term  $n = 0$  in the second sum in (9), we obtain, making use of AI(4a)

$$k_1(\mathbf{x}) - k_2(\mathbf{x}) = K\left(\frac{2\mathbf{x}}{1+M}\right) \exp\left(i \frac{1-M}{1+M} \mathbf{x}\right) + \dots$$

Finally

$$\begin{aligned} k(\mathbf{x}) &= K\left(\frac{2\mathbf{x}}{1+M}\right) \exp\left(i \frac{1-M}{1+M} \mathbf{x}\right) \\ &\quad - \left( \frac{i}{2\mathbf{x}} \right)^{0.5} \sum_{n=1}^{\infty} C_n \left( i \frac{1-M^2}{2M\mathbf{x}} \right)^n \exp\left(-\frac{iM\mathbf{x}}{1+M}\right) \dots \dots \dots \quad (12) \end{aligned}$$

with the coefficients

$$C_n = \frac{\bar{n}!}{\pi} \sqrt{\frac{M}{\pi}} \left[ \frac{1}{n-1} - \frac{1+M}{2M} \sum_0^{\infty} \frac{1}{m+n} \left( \frac{M-1}{2M} \right)^m \right] \dots \dots \quad (12a)$$

and

$$k(-\mathbf{x}) = \left( \frac{i}{2\mathbf{x}} \right)^{0.5} \sum_1^{\infty} D_n \left( i \frac{1-M^2}{2M\mathbf{x}} \right)^n \exp\left(-\frac{iM\mathbf{x}}{1-M}\right) \dots \dots \dots \quad (13)$$

where

$$D_n = \frac{\bar{n}!}{\pi} \sqrt{\frac{M}{\pi}} \sum_0^{n-1} \frac{\bar{m}}{1-2m} \left( \frac{2M}{1+M} \right)^{n-m} \dots \dots \dots \quad (13a)$$

The set of formulae† (11), (12), (13) is convenient for numerical evaluation if  $\kappa/\mathbf{x}$  is sufficiently small.

† This set has been checked by using it for recalculating some of Schade's values<sup>18</sup>.



APPENDIX IV

Part Solution for  $M = 1 - \delta$

The modified Possio equation as defined in section 3.5.3 becomes for the elementary downwash  $w_r$  (see 3.4.2(9))

$$y^r = \frac{1}{\alpha} \int_0^{\bar{y}} d\bar{\eta} e^{-M\bar{\eta}} (\bar{\eta})^{-0.5} \phi_r(y - \eta) \sum_0^{\infty} \frac{(-\bar{\eta})^n}{\bar{n}!} \dots \dots \dots \dots \quad (1)$$

if

$$\alpha = \frac{2}{1 + M}; \quad \bar{y} = \alpha y = \frac{\omega x}{1 + M}; \quad \bar{\eta} = \alpha \eta \dots \dots \dots \dots \quad (1a)$$

(compare 3.5.2(6)). We introduce a function  $P_r$  defined by a relation similar to 3.5.2(7) :

$$P_r = (\bar{y})^{r-0.5} e^{-\bar{y}} \sum_0^{\infty} \frac{(\bar{y})^n}{n!} \frac{2n + r}{n + r} \dots \dots \dots \dots \quad (2)$$

Substituting  $P_r$  for  $\phi_r$  in (1) leads to

$$R(y) = \frac{1}{\alpha} (\bar{y})^r e^{(1-M)\bar{y}}$$

(compare 3.5.2(8), (9), (10)) ; it follows that

$$\phi_r = \alpha^{1-r} \sum_{m=0}^{\infty} P_{r+m} \frac{(M-1)^n}{n!} \dots \dots \dots \dots \quad (3)$$

is the solution of (1). After some manipulation

$$\phi_r = \frac{r! \alpha^{1-r}}{M(\pi y)^{0.5}} w_r \sum_0^{\infty} \bar{n} \frac{(-\bar{y}M)^n}{r + n!} \frac{M + 2n}{1 - 2n} \dots \dots \dots \dots \quad (3a)$$

The limit of (3a) as  $M$  tends to unity agrees with 3.4.2(11), as of course it should.

Substituting (3a) in 3.4.3(14) we find

$$l_z^n = \frac{1}{(n-1)!(2n-3)} \alpha^{n-0.5} M^{n-2} \left( 1 - \frac{1-M}{2n-1} \right) \dots \dots \dots \dots \quad (4)$$

(compare 3.4.1 (2a)). 3.4.1(2b) remains valid. The derivatives with respect to  $M$  of the modified forces can immediately be written down. Defining, in accordance with 3.4.1(2), for the point  $M = 1$

$$\left( \frac{\partial l_z}{\partial M} \right)_{M=1} = \frac{8}{(2\pi\omega)^{0.5}} \sum_0^{\infty} \left( \frac{\partial l_z^n}{\partial M} \right)_{M=1} \left( -\frac{\omega}{2} \right)^n$$

we find

$$\left( \frac{\partial l_z^n}{\partial M} \right)_{M=1} = \left( \frac{2n-7}{4} + \frac{1}{2n-1} \right) l_z^n \dots \dots \dots \dots \quad (5)$$

The derivatives of the other series coefficients, are given by relations which may be obtained from 3.4.1(2b) by replacing all the series coefficients by their derivatives with respect to  $M$ . It follows that

$$\left. \begin{aligned} - \left( \frac{\partial l_z}{\partial M} \right)_{M=1} &= \frac{1-i}{\sqrt{(\pi\nu)}} \left( 0 + \frac{1}{2} i\nu - \frac{5}{12} \nu^2 \dots \right) \\ - \left( \frac{\partial l_a}{\partial M} \right)_{M=1} &= \frac{1-i}{\sqrt{(\pi\nu)}} \left( \frac{1}{2} + \frac{3}{4} i\nu - \frac{39}{240} \nu^2 \dots \right) \end{aligned} \right\} \dots \dots \dots \dots \quad (6)$$

TABLE 1

*Comparison of Different Notations for Leading-edge Derivatives*

Present report	British <sup>16</sup> subsonic	Temple and Jahn <sup>7</sup> supersonic	Küssner, subsonic	Jordan <sup>13</sup> supersonic
$l_z$	$l_z + ivl_z - v^2 l_z$	$l_z + ivl_z$	$\pi k_a$	$\pi k_a$
$l_a$	$l_a + ivl_a - v^2 l_a$	$l_a + ivl_a + \frac{1}{2}(l_z + ivl_z)$	$\frac{1}{2}\pi(k_b + \frac{1}{2}k_a)$	$\frac{1}{2}\pi k_b$
$m_z$	$m_z + ivm_z - v^2 m_z$	$m_z + ivm_z - \frac{1}{2}(l_z + ivl_z)$	$-\frac{1}{2}\pi(m_a + \frac{1}{2}k_a)$	$-\frac{1}{2}\pi m_a$
$m_a$	$m_a + ivm_a - v^2 m_a$	$m_a + ivm_a - \frac{1}{4}(l_z + ivl_z) + \frac{1}{2}(m_z + ivm_z - l_a - ivl_a)$	$-\frac{1}{4}\pi\{(m_b + \frac{1}{4}k_a + \frac{1}{2}(m_a + k_b))\}$	$-\frac{1}{4}\pi m_b$

TABLE 2

Wing Force Coefficients

2a Lift coefficient  $l_z = l_z' + il_z''$

$\alpha$	$M$														
	0	0.5	0.6	0.7	0.8	0.9	0.95	1.0	1.05	1.1111	1.1765	1.25	1.4286	1.6667	2.0
0	0	0	0	0	0	0	0	0	0	0	0	0	0	0	0
0.05	+0.0117	+0.01878	+0.0236	+0.0320	0.055	0.115	0.169	0.2460	0.0720	0.0217	0.0104	0.0059	0.0024	0.0011	0.0005
0.1	0.0333	0.05214	0.0645	0.0844	0.123	0.198	0.258	0.3391	0.237	0.0833	0.0409	0.0234	0.0093	0.0042	0.0019
0.15	0.0561	0.0879	0.1072	0.1377	0.188	0.270	0.330	0.4047	0.402	0.1747	0.0892	0.0516	0.0208	0.0094	0.0043
0.2	0.0768	0.1206	0.1460	0.1849	0.243	0.330	0.387	0.4550	0.480	0.2817	0.1517	0.0893	0.0366	0.0166	0.0076
0.25	0.0936	0.1484	0.1787	0.2240	0.289	0.377	0.432	0.4952	0.470	0.3880	0.2236	0.1349	0.0563	0.0256	0.0118
0.3	0.1050	0.1696	0.2043	0.2555	0.326	0.417	0.470	0.5276	0.437	0.4788	0.2998	0.1864	0.0794	0.0365	0.0168
0.35	0.1110	0.1844	0.2232	0.2798	0.356	0.449	0.501	0.5543	0.446	0.5432	0.3750	0.2415	0.1056	0.0489	0.0227
0.4	0.1114	0.1929	0.2356	0.2975	0.379	0.475	0.526	0.5759	0.5069	0.5760	0.4441	0.2979	0.1342	0.0628	0.0293
0.5	0.0946	0.1922	0.2424	0.3150	0.408	0.512	0.562	0.6071	0.6034	0.5574	0.5474	0.4052	0.1962	0.0943	0.0444
0.6	+0.0553	0.1690	0.2271	0.3120	0.419	0.534	0.585	0.6257	0.5421	0.488	0.5889	0.4915	0.2602	0.1291	0.0618
0.7	-0.0059	0.1251	0.1925	0.2935	0.420	0.549	0.601	0.6342	0.5705	0.449	0.5695	0.5444	0.3210	0.1654	0.0805
0.8	-0.0880	+0.0616	0.1404	0.2614	0.412	0.558	0.611	0.6345	0.6202	0.479	0.5091	0.5584	0.3735	0.2014	0.1001
0.9	-0.1902	-0.0202	+0.0726	0.2186	0.400	0.566	0.618	0.6279	0.5494	0.542	0.438	0.5355	0.4134	0.2350	0.1197
1.0	-0.3119	-0.1191	-0.0088	0.1678	0.385	0.576	0.625	0.6155	0.5557	0.576	0.383	0.4840	0.4377	0.2644	0.1385
1.2	-0.6115	-0.3629	-0.2061	+0.0622	0.389	0.642	0.670	0.5765	0.5032	0.47	0.374	0.348	0.4337	0.3045	0.1707
1.4	-0.9834	-0.6641	-0.4373	-0.0418	0.431	0.756	0.743	0.5227	0.5039	0.38	0.429	0.250	0.3648	0.3122	0.1912

34

$l_z'$

TABLE 2a

2a Lift coefficient  $l_z = l_z' + il_z''$ 

35

$\nu$	$M$														
	0	0.5	0.6	0.7	0.8	0.9	0.95	1.0	1.05	1.1111	1.1765	1.25	1.4286	1.6667	2.0
0	0	0	0	0	0	0	0	0	0	0	0	0	0	0	0
0.05	0.1499	0.1699	0.1816	0.1989	0.221	0.243	0.252	0.2587	0.2926	0.2036	0.1604	0.1329	0.0979	0.0750	0.0577
0.1	0.2855	0.3175	0.3353	0.3595	0.384	0.397	0.392	0.3748	0.485	0.3906	0.3153	0.2634	0.1951	0.1497	0.1153
0.15	0.4090	0.4478	0.4678	0.4938	0.517	0.519	0.504	0.4701	0.551	0.5475	0.4595	0.3891	0.2910	0.2239	0.1728
0.2	0.5227	0.5649	0.5856	0.6107	0.630	0.623	0.600	0.5559	0.548	0.6660	0.5888	0.5080	0.3848	0.2974	0.2299
0.25	0.6286	0.6702	0.6908	0.7138	0.728	0.714	0.685	0.6361	0.567	0.7448	0.7001	0.6181	0.4761	0.3699	0.2867
0.3	0.7283	0.7708	0.7912	0.8128	0.824	0.802	0.769	0.7131	0.653	0.7889	0.7922	0.7184	0.5641	0.4413	0.3430
0.35	0.8232	0.8673	0.8876	0.9085	0.917	0.890	0.851	0.7877	0.781	0.8092	0.8646	0.8077	0.6486	0.5113	0.3988
0.4	0.9143	0.9604	0.9808	1.0015	1.008	0.975	0.932	0.8609	0.8902	0.8191	0.9190	0.8856	0.7290	0.5798	0.4539
0.5	1.0879	1.1389	1.1605	1.1825	1.188	1.146	1.092	1.0053	0.9622	0.8606	0.9860	1.0085	0.8767	0.7113	0.5620
0.6	1.2534	1.3116	1.3361	1.3616	1.368	1.317	1.253	1.1485	1.0754	0.983	1.0256	1.0934	1.0058	0.8351	0.6668
0.7	1.4138	1.4853	1.5155	1.5463	1.554	1.493	1.416	1.2923	1.2847	1.177	1.0744	1.1532	1.1166	0.9505	0.7679
0.8	1.5707	1.6606	1.6990	1.7373	1.747	1.675	1.584	1.4376	1.3717	1.376	1.1600	1.2041	1.2108	1.0570	0.8651
0.9	1.7254	1.8397	1.8891	1.9371	1.950	1.865	1.757	1.5848	1.4959	1.519	1.293	1.2623	1.2914	1.1551	0.9582
1.0	1.8785	2.0248	2.0879	2.1482	2.165	2.066	1.938	1.7345	1.6985	1.604	1.465	1.3408	1.3627	1.2456	1.0472
1.2	2.1820	2.4175	2.5177	2.5924	2.594	2.447	2.286	2.0421	1.9357	1.81	1.834	1.585	1.4965	1.4075	1.2137
1.4	2.4839	2.8510	2.9961	3.0753	3.039	2.825	2.630	2.3618	2.2536	2.18	2.109	1.923	1.6498	1.5550	1.3681

 $l_z''$

TABLE 2b

Lift coefficient  $l_a$

$\nu$	$M$														
	0	0.5	0.6	0.7	0.8	0.9	0.95	1.0	1.05	1.1111	1.1765	1.25	1.4286	1.6667	2.0
0	3.1416	3.6276	3.9270	4.3992	5.236	7.207	10.061	$\infty$	6.247	4.1295	3.2272	2.6667	1.9604	1.5000	1.1547
0.05	3.0073	3.4129	3.6518	4.0022	4.448	4.932	5.155	5.3386	5.877	4.0794	3.2118	2.6603	1.9589	1.4995	1.1545
0.1	2.8823	3.2186	3.4004	3.6611	3.944	4.124	4.111	3.9789	4.939	3.9347	3.1666	2.6419	1.9544	1.4981	1.1541
0.15	2.7734	3.0572	3.2045	3.4031	3.597	3.667	3.597	3.4130	3.840	3.7113	3.0935	2.6116	1.9467	1.4957	1.1533
0.2	2.6791	2.9251	3.0499	3.2092	3.351	3.372	3.285	3.0960	2.977	3.4330	2.9966	2.5705	1.9365	1.4926	1.1522
0.25	2.5968	2.8209	2.9318	3.0701	3.186	3.182	3.086	2.8929	2.552	3.1286	2.8802	2.5196	1.9233	1.4883	1.1506
0.3	2.5243	2.7308	2.8315	2.9548	3.054	3.037	2.941	2.7523	2.487	2.8268	2.7503	2.4602	1.9076	1.4833	1.1490
0.35	2.4593	2.6534	2.7472	2.8608	2.950	2.927	2.832	2.6498	2.562	2.5541	2.6127	2.3944	1.8897	1.4775	1.1470
0.4	2.4007	2.5873	2.6771	2.7857	2.870	2.845	2.751	2.5724	2.5747	2.3298	2.4734	2.3237	1.8694	1.4709	1.1448
0.5	2.2957	2.4827	2.5724	2.6828	2.770	2.745	2.649	2.4651	2.3177	2.0618	2.2128	2.1752	1.8239	1.4555	1.1393
0.6	2.2012	2.4052	2.5031	2.6268	2.727	2.705	2.600	2.3960	2.2162	2.010	2.0056	2.0293	1.7733	1.4379	1.1329
0.7	2.1115	2.3392	2.4500	2.5921	2.710	2.691	2.576	2.3492	2.2761	2.065	1.8721	1.8994	1.7197	1.4183	1.1258
0.8	2.0231	2.2841	2.4128	2.5789	2.718	2.703	2.574	2.3165	2.1761	2.113	1.8130	1.7948	1.6660	1.3971	1.1178
0.9	1.9334	2.2354	2.3863	2.5811	2.746	2.733	2.587	2.2929	2.1377	2.094	1.812	1.7211	1.6143	1.3752	1.1091
1.0	1.8409	2.1888	2.3653	2.5925	2.786	2.776	2.610	2.2755	2.1807	2.027	1.844	1.6789	1.5669	1.3531	1.1002
1.2	1.6424	2.1067	2.3502	2.6496	2.897	2.882	2.673	2.2522	2.1083	1.95	1.905	1.672	1.4907	1.3104	1.0817
1.4	1.4216	2.0367	2.3601	2.7320	3.024	2.992	2.737..	2.2374	2.1054	2.00	1.887	1.716	1.4451	1.2731	1.0631

96

$l_a'$

TABLE 2b—continued

Lift coefficient  $l_a$

37

$\nu$	$M$														
	0	0.5	0.6	0.7	0.8	0.9	0.95	1.0	1.05	1.1111	1.1765	1.25	1.4286	1.6667	2.0
0	0	0	0	0	0	0	0	—	0	0	0	0	0	0	0
0.05	-0.1213	-0.2445	-0.3318	-0.4830	-0.934	-2.122	-3.199	-4.7499	-1.286	-0.3315	-0.1283	-0.0515	0.0020	0.0164	0.0193
0.1	-0.1184	-0.2849	-0.3929	-0.5790	-0.954	-1.711	-2.320	-3.1463	-2.098	-0.6318	-0.2500	-0.1010	0.0043	0.0329	0.0385
0.15	-0.0671	-0.2509	-0.3649	-0.5513	-0.874	-1.436	-1.853	-2.3932	-2.327	-0.8737	-0.3591	-0.1465	0.0073	0.0496	0.0578
0.2	+0.0078	-0.1797	-0.2931	-0.4708	-0.754	-1.207	-1.523	-1.9183	-1.992	-1.0375	-0.4501	-0.1863	0.0112	0.0665	0.0772
0.25	0.0971	-0.0834	-0.1914	-0.3586	-0.615	-1.001	-1.261	-1.5759	-1.445	-1.1135	-0.5186	-0.2186	0.0165	0.0836	0.0967
0.3	0.1961	+0.0179	-0.0854	-0.2440	-0.480	-0.823	-1.046	-1.3093	-0.994	-1.1023	-0.5617	-0.2422	0.0233	0.1012	0.1162
0.35	0.3002	0.1235	+0.0242	-0.1277	-0.350	-0.663	-0.861	-1.0909	-0.773	-1.0144	-0.5779	-2.2559	0.0319	0.1192	0.1359
0.4	0.4073	0.2327	0.1367	-0.0102	-0.223	-0.516	-0.698	-0.9055	-0.7249	-0.8680	-0.5664	-0.2589	0.0426	0.1378	0.1558
0.5	0.6268	0.4587	0.3675	+0.2256	+0.022	-0.252	-0.417	-0.6003	-0.5853	-0.4901	-0.4685	-0.2318	0.0709	0.1766	0.1959
0.6	0.8480	0.6898	0.6014	0.4583	0.252	-0.021	-0.180	-0.3517	-0.2183	-0.140	-0.2919	-0.1613	0.1095	0.2181	0.2369
0.7	1.0688	0.9167	0.8300	0.6803	0.462	+0.180	+0.023	-0.1392	-0.0585	+0.089	-0.0728	-0.0531	0.1589	0.2627	0.2787
0.8	1.2881	1.1432	1.0562	0.8944	0.656	0.358	0.200	+0.0484	+0.0538	0.201	+0.1510	+0.0833	0.2190	0.3104	0.3215
0.9	1.5054	1.3701	1.2801	1.1006	0.834	0.515	0.357	0.2183	0.2844	0.269	0.350	0.2364	0.2895	0.3616	0.3654
1.0	1.7208	1.5979	1.5018	1.2990	0.999	0.653	0.496	0.3748	0.4097	0.365	0.507	0.3942	0.3690	0.4162	0.4104
1.2	2.1461	2.0530	1.9434	1.6641	1.251	0.832	0.693	0.6594	0.6863	0.68	0.705	0.684	0.5491	0.5349	0.5038
1.4	+2.5654	+2.5151	+2.3770	+1.9873	+1.422	+0.915	+0.814	+0.9180	+0.8908	+0.92	+0.849	+0.906	0.7440	0.6647	0.6017

$l_a''$

TABLE 2c

Moment coefficient  $m_x$

$\nu$	$M$														
	0	0.5	0.6	0.7	0.8	0.9	0.95	1.0	1.05	1.1111	1.1765	1.25	1.4286	1.6667	2.0
0	0	0	0	0	0	0	0	0	0	0	0	0	0	0	0
0.05	+0.0024	+0.0040	+0.0050	+0.0068	+0.014	+0.034	+0.053	+0.0803	0.0474	+0.0144	+0.0069	+0.0039	0.0016	0.0007	0.0003
0.1	0.0064	0.0102	0.0126	0.0165	0.027	0.053	0.076	0.1083	0.151	0.0549	0.0272	0.0155	0.0062	0.0028	0.0013
0.15	0.0096	0.0156	0.0192	0.0246	0.037	0.066	0.091	0.1263	0.235	0.1135	0.0588	0.0341	0.0139	0.0063	0.0029
0.2	0.0114	0.0191	0.0233	0.0296	0.043	0.074	0.101	0.1385	0.242	0.1788	0.0990	0.0588	0.0243	0.0110	0.0051
0.25	0.0111	0.0201	0.0245	0.0310	0.045	0.078	0.107	0.1468	0.183	0.2386	0.1440	0.0882	0.0372	0.0170	0.0078
0.3	0.0086	0.0182	0.0227	0.0291	0.044	0.078	0.109	0.1521	0.123	0.2817	0.1900	0.1207	0.0522	0.0241	0.0112
0.35	+0.0037	0.0136	0.0179	0.0240	0.039	0.076	0.108	0.1550	0.114	0.3009	0.2326	0.1547	0.0691	0.0323	0.0150
0.4	-0.0036	+0.0062	+0.0102	+0.0157	0.031	0.069	0.105	0.1558	0.1577	0.2938	0.2681	0.1882	0.0873	0.0413	0.0193
0.5	-0.0254	-0.0168	-0.0137	-0.0096	+0.005	0.049	0.091	0.1525	0.2102	0.2167	0.3066	0.2470	0.1257	0.0614	0.0291
0.6	-0.0569	-0.0502	-0.0485	-0.0457	-0.030	+0.021	0.071	0.1440	0.1182	0.116	0.2926	0.2845	0.1635	0.0831	0.0402
0.7	-0.0977	-0.0938	-0.0937	-0.0914	-0.073	-0.013	0.045	0.1312	0.1296	0.065	0.2322	0.2925	0.1965	0.1050	0.0519
0.8	-0.1477	-0.1473	-0.1487	-0.1461	-0.124	-0.052	+0.016	0.1150	0.1586	0.085	0.1462	0.2687	0.2210	0.1256	0.0638
0.9	-0.2066	-0.2105	-0.2131	-0.2088	-0.180	-0.095	-0.017	0.0959	0.0738	0.136	0.062	0.2169	0.2340	0.1433	0.0752
1.0	-0.2743	-0.2832	-0.2865	-0.2787	-0.241	-0.140	-0.051	0.0745	0.0736	0.154	+0.005	+0.1461	0.2336	0.1568	0.0855
1.2	-0.4356	-0.4558	-0.4584	-0.4258	-0.344	-0.197	-0.096	+0.0261	0.0080	+0.03	-0.020	-0.003	0.1900	0.1670	0.1006
1.4	-0.6307	-0.6647	-0.6594	-0.5795	-0.424	-0.218	-0.115	-0.0277	0.0082	-0.05	+0.049	-0.093	0.0984	0.1499	0.1052

88

$-m_x'$

TABLE 2c—continued

Moment coefficient  $m_z$ 

$\nu$	$M$														
	0	0.5	0.6	0.7	0.8	0.9	0.95	1.0	1.05	1.1111	1.1765	1.25	1.4286	1.6667	2.0
0	0	0	0	0	0	0	0	0	0	0	0	0	0	0	0
0.05	0.0375	0.0425	0.0455	0.0499	0.057	0.069	0.077	0.0879	0.1414	0.1011	0.0800	0.0664	0.0489	0.0375	0.0289
0.1	0.0714	0.0796	0.0842	0.0907	0.100	0.112	0.120	0.1298	0.209	0.1898	0.1558	0.1309	0.0973	0.0748	0.0576
0.15	0.1023	0.1125	0.1180	0.1257	0.136	0.149	0.157	0.1656	0.191	0.2563	0.2237	0.1919	0.1447	0.1117	0.0863
0.2	0.1307	0.1423	0.1485	0.1569	0.168	0.182	0.190	0.1991	0.140	0.2951	0.2805	0.2477	0.1906	0.1480	0.1147
0.25	0.1572	0.1694	0.1762	0.1853	0.197	0.212	0.221	0.2314	0.131	0.3063	0.3244	0.2972	0.2345	0.1837	0.1428
0.3	0.1821	0.1954	0.2030	0.2133	0.227	0.243	0.253	0.2632	0.188	0.2953	0.3543	0.3394	0.2762	0.2185	0.1707
0.35	0.2058	0.2206	0.2291	0.2409	0.256	0.275	0.285	0.2950	0.281	0.2717	0.3708	0.3737	0.3151	0.2523	0.1981
0.4	0.2286	0.2451	0.2546	0.2685	0.287	0.307	0.317	0.3268	0.3478	0.2470	0.3753	0.3999	0.3511	0.2849	0.2250
0.5	0.2720	0.2928	0.3051	0.3244	0.349	0.375	0.385	0.3912	0.3407	0.2359	0.3597	0.4298	0.4135	0.3462	0.2772
0.6	0.3134	0.3400	0.3562	0.3831	0.417	0.448	0.457	0.4574	0.3903	0.310	0.3360	0.4356	0.4627	0.4019	0.3270
0.7	0.3535	0.3883	0.4101	0.4467	0.492	0.528	0.534	0.5256	0.5282	0.446	0.3336	0.4287	0.4992	0.4514	0.3742
0.8	0.3927	0.4382	0.4672	0.5164	0.575	0.618	0.619	0.5961	0.5426	0.576	0.3727	0.4227	0.5250	0.4948	0.4184
0.9	0.4313	0.4903	0.5284	0.5934	0.669	0.718	0.711	0.6689	0.6011	0.647	0.458	0.4308	0.5427	0.5324	0.4599
1.0	0.4696	0.5454	0.5947	0.6792	0.776	0.830	0.813	0.7443	0.7331	0.663	0.576	0.4628	0.5561	0.5650	0.4984
1.2	0.5455	0.6669	0.7473	0.8773	1.018	1.079	1.033	0.9024	0.8301	0.74	0.817	0.611	0.5859	0.6191	0.5679
1.4	0.6210	0.8090	0.9309	1.1179	1.309	1.371	1.285	1.0704	1.0028	0.99	0.954	0.838	0.6452	0.6675	0.6297

— $m_z''$



TABLE 2d

Moment coefficient  $m_a$

$\nu$	$M$														
	0	0.5	0.6	0.7	0.8	0.9	0.95	1.0	1.05	1.1111	1.1765	1.25	1.4286	1.6667	2.0
0	0.7854	0.9069	0.9818	1.0998	1.309	1.802	2.515	$\infty$	3.124	2.0647	1.6136	1.3334	0.9802	0.7500	0.5773
0.05	0.7515	0.8535	0.9138	1.0029	1.151	1.409	1.603	1.8573	2.850	2.0272	1.6021	1.3287	0.9791	0.7497	0.5773
0.1	0.7193	0.8049	0.8520	0.9212	1.026	1.187	1.298	1.4352	2.162	1.9192	1.5682	1.3148	0.9756	0.7486	0.5769
0.15	0.6906	0.7641	0.8037	0.8597	0.943	1.071	1.160	1.2697	1.397	1.7540	1.5138	1.2921	0.9700	0.7468	0.5762
0.2	0.6649	0.7300	0.7650	0.8138	0.887	1.001	1.082	1.1830	0.870	1.5514	1.4420	1.2614	0.9623	0.7444	0.5755
0.25	0.6415	0.7022	0.7348	0.7805	0.849	0.958	1.035	1.1315	0.713	1.3345	1.3565	1.2237	0.9525	0.7413	0.5744
0.3	0.6200	0.6772	0.7082	0.7525	0.820	0.927	1.003	1.0987	0.829	1.1270	1.2623	1.1801	0.9408	0.7376	0.5731
0.35	0.5998	0.6547	0.6849	0.7292	0.798	0.906	0.982	1.0771	1.009	0.9494	1.1639	1.1319	0.9276	0.7332	0.5715
0.4	0.5805	0.6343	0.6645	0.7100	0.781	0.891	0.967	1.0627	1.0836	0.8159	1.0664	1.0806	0.9126	0.7283	0.5699
0.5	0.5432	0.5984	0.6306	0.6822	0.761	0.878	0.955	1.0466	0.9212	0.7022	0.8919	0.9752	0.8792	0.7170	0.5658
0.6	0.5061	0.5668	0.6033	0.6651	0.757	0.883	0.958	1.0401	0.9049	0.757	0.7674	0.8752	0.8423	0.7039	0.5611
0.7	0.4678	0.5358	0.5781	0.6531	0.762	0.897	0.969	1.0386	1.0137	0.875	0.7064	0.7913	0.8042	0.6895	0.5558
0.8	0.4272	0.5051	0.5551	0.6469	0.776	0.922	0.988	1.0398	0.9477	0.956	0.7052	0.7305	0.7667	0.6742	0.5499
0.9	0.3840	0.4736	0.5333	0.6459	0.800	0.957	1.015	1.0424	0.9424	0.959	0.755	0.6960	0.7318	0.6586	0.5437
1.0	0.3375	0.4401	0.5117	0.6492	0.833	1.002	1.050	1.0456	1.0069	0.911	0.808	0.6873	0.7010	0.6431	0.5371
1.2	0.2339	0.3704	0.4737	0.6725	0.925	1.120	1.136	1.0525	0.9673	0.87	0.898	0.729	0.6564	0.6141	0.5240
1.4	0.1149	0.2978	0.4424	0.7213	1.062	1.285	1.255	1.0583	0.9850	0.95	0.895	0.799	0.6378	0.5902	0.5113

40

$-m_a'$

TABLE 2d—continued

Moment coefficient  $m_a$

$\nu$	$M$														
	0	0.5	0.6	0.7	0.8	0.9	0.95	1.0	1.05	1.1111	1.1765	1.25	1.4286	1.6667	2.0
0	0	0	0	0	0	0	0	—	0	0	0	0	0	0	0
0.05	-0.0107	-0.0350	-0.0522	-0.0819	-0.210	-0.596	-0.964	-1.5040	-0.847	-0.2203	-0.0854	-0.0343	0.0013	0.0109	0.0128
0.1	+0.0097	-0.0196	-0.0382	-0.0700	-0.163	-0.404	-0.622	-0.9356	-1.326	-0.4157	-0.1655	-0.0670	0.0029	0.0220	0.0257
0.15	0.0421	+0.0140	-0.0026	-0.0292	-0.100	-0.276	-0.433	-0.6578	-1.338	-0.5647	-0.2356	-0.0965	0.0050	0.0331	0.0386
0.2	0.0805	0.0566	+0.0435	+0.0241	-0.029	-0.168	-0.294	-0.4763	-0.982	-0.6523	-0.2912	-0.1214	0.0079	0.0444	0.0515
0.25	0.1224	0.1052	0.0967	0.0844	+0.044	-0.073	-0.182	-0.3412	-0.469	-0.6717	-0.3292	-0.1404	0.0119	0.0560	0.0645
0.3	0.1668	0.1551	0.1509	0.1454	0.115	+0.014	-0.085	-0.2328	-0.139	-0.6252	-0.3472	-0.1525	0.0171	0.0678	0.0776
0.35	0.2125	0.2062	0.2061	0.2070	0.185	0.094	+0.001	-0.1416	-0.031	-0.5229	-0.3442	-0.1568	0.0237	0.0801	0.0908
0.4	0.2589	0.2583	0.2621	0.2692	0.255	0.171	0.080	-0.0622	-0.0701	-0.3811	-0.3204	-0.1528	0.0319	0.0927	0.1041
0.5	0.3530	0.3648	0.3762	0.3948	0.393	0.317	0.223	+0.0729	-0.0439	-0.0568	-0.2168	-0.1191	0.0540	0.1194	0.1311
0.6	0.4476	0.4731	0.4923	0.5214	0.529	0.453	0.352	0.1874	+0.2180	+0.207	-0.0586	-0.0527	0.0840	0.1482	0.1587
0.7	0.5421	0.5810	0.6087	0.6480	0.663	0.583	0.473	0.2887	0.2772	0.345	+0.1226	+0.0411	0.1224	0.1793	0.1870
0.8	0.6362	0.6900	0.7264	0.7750	0.796	0.709	0.586	0.3809	0.3125	0.379	0.2957	0.1537	0.1690	0.2130	0.2161
0.9	0.7298	0.8006	0.8455	0.9025	0.927	0.830	0.694	0.4667	0.4708	0.386	0.437	0.2752	0.2232	0.2494	0.2460
1.0	0.8229	0.9135	0.9663	1.0304	1.056	0.948	0.797	0.5476	0.5265	0.430	0.537	0.3955	0.2841	0.2882	0.2768
1.2	1.0078	1.1430	1.2160	1.2824	1.290	1.145	0.971	0.6993	0.6865	0.64	0.631	0.601	0.4197	0.3733	0.3410
1.4	+1.1911	+1.3824	+1.4729	+1.5245	+1.489	+1.295	+1.109	+0.8420	+0.7854	+0.79	+0.691	+0.739	0.5631	0.4663	0.4087

41

— $m_a''$

TABLE 3

*Additional Values for  $M = 1.0$  and  $M = 1.05$* 

	$\nu$	$l_z'$	$l_z''$	$l_a'$	$l_a''$	$-m_z'$	$-m_z''$	$-m_a'$	$-m_a''$
$M = 1.0$	1.6	0.4582	2.6940	2.2268	1.1594	-0.0848	1.2482	1.0625	0.9791
	1.8	0.3859	3.0390	2.2180	1.3891	-0.1437	1.4354	1.0648	1.1126
	2.0	0.3084	3.3965	2.2097	1.6107	-0.2030	1.6316	1.0653	1.2439
$M = 1.05$	1.6	0.4086	2.6079	2.1183	1.1406	-0.0797	1.2119	1.0142	0.9388
	1.8	0.3252	2.8935	2.0850	1.3647	-0.1523	1.3481	0.9928	1.0750
	2.0	0.2951	3.2441	2.0825	1.5524	-0.1653	1.5441	0.9987	1.1788

TABLE 4

*Coefficients for  $M = 0.8$  by Schade<sup>20</sup> and Timman<sup>21</sup>*

		$l_z'$	$l_z''$	$l_a'$	$l_a''$	$-m_z'$	$-m_z''$	$-m_a'$	$-m_a''$
Schade	0.4	0.3886	1.0119	2.8897	-0.2549	0.0263	0.2899	0.7838	0.2719
	0.8	0.4514	1.7194	2.7062	+0.5543	-0.1086	0.5938	0.8260	0.7876
	1.2	0.4263	2.4460	2.7207	1.0714	-0.2571	1.0133	0.9982	1.1641
	1.6	0.2900	3.1325	2.6148	+1.5095	-0.3585	1.4358	1.1051	1.3819
Timman	0.2	0.2596	0.6412	3.3805	-0.8326	0.0419	0.1702	0.8833	-0.0202
	0.3	0.3549	0.8249	3.0821	-0.5854	0.0445	0.2287	0.8235	+0.1178
	0.4	0.4242	0.9971	2.8746	-0.3513	0.0343	0.2889	0.7864	0.2542
	0.5	0.4713	1.1612	2.7408	-0.1302	0.0137	0.3523	0.7690	0.3882
	0.6	0.5003	1.3209	2.6638	+0.0781	-0.0152	0.4204	0.7681	0.5187
	0.8	0.5190	1.6411	2.6123	0.4562	-0.0892	0.5759	0.8041	0.7660
	1.0	0.5116	1.9860	2.5845	0.7837	-0.1701	0.7669	0.8704	0.9890
	1.2	0.4900	2.3430	2.6106	1.0675	-0.2381	0.9802	0.9618	1.1683
	1.4	0.4669	2.7084	2.6432	+1.3084	-0.2856	1.1994	1.0490	+1.2998

TABLE 5

*Errata in Temple-Jahn<sup>7</sup>*

$y$	$\lambda$	$l_z$	$-m_a$	$l_a$	$-m_z$
3.0	0.2789	0.4483		-5.233	
3.5	0.3254	0.4335	-0.2822	-3.715	-0.3789
3.8	0.3533	0.4481	-0.2106	-3.284	
4.0	0.3719	0.4676	-0.1790	-3.110	-0.2715

TABLE 6

*Possio kernel  $k(\mathbf{x})$  and modified kernel  $k_0(\mathbf{x})$* *(see sections 3.5.1 and 3.5.3)*

$x$	$M = 0.9$				$M = 1.0$	
	$k'$	$k''$	$k_0'$	$k_0''$	$k' \equiv k_0'$	$k'' \equiv k_0''$
0.05	1.9264	+0.8134	1.3204	+1.1328	1.3531	+1.1640
0.1	1.2188	0.5744	0.9933	0.7286	1.0170	0.7501
0.2	0.8541	0.3358	0.7766	0.4050	0.7940	0.4194
0.3	0.7226	+0.1912	0.6828	0.2335	0.6976	0.2445
0.4	0.6466	+0.0835	0.6225	0.1131	0.6358	0.1220
0.5	0.5904	-0.0043	0.5744	+0.0181	0.5866	+0.0254
0.6	0.5419	-0.0790	0.5307	-0.0612	0.5422	-0.0550
0.7	0.4961	-0.1439	0.4880	-0.1293	0.4989	-0.1241
0.8	0.4508	-0.2008	0.4448	-0.1885	0.4552	-0.1841
0.9	0.4047	-0.2506	0.4003	-0.2401	0.4103	-0.2364
1.0	0.3575	-0.2939	0.3541	-0.2847	0.3638	-0.2818
1.1	0.3088	-0.3310	0.3063	-0.3229	0.3157	-0.3205
1.2	0.2589	-0.3621	0.2571	-0.3549	0.2661	-0.3530
1.3	0.2079	-0.3872	0.2066	-0.3807	0.2153	-0.3794
1.4	0.1561	-0.4065	0.1552	-0.4006	0.1637	-0.3998
1.5	0.1038	-0.4200	0.1033	-0.4147	0.1115	-0.4142

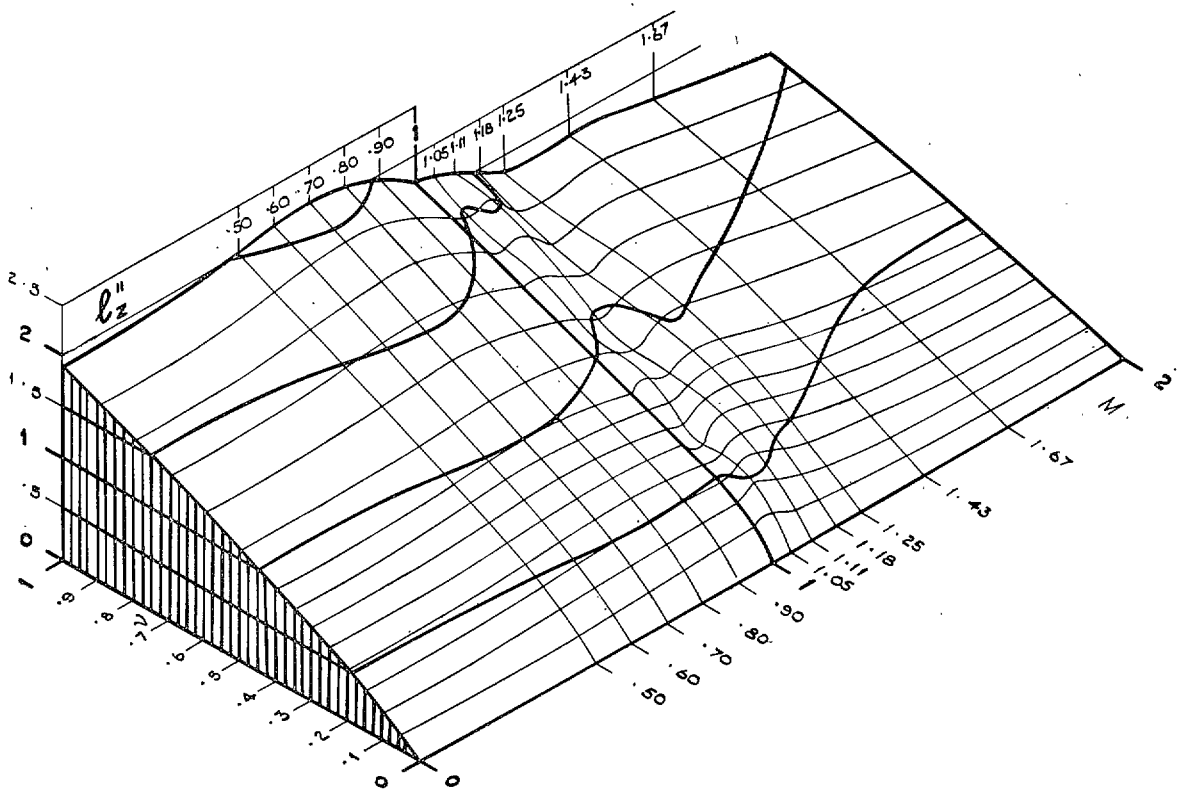
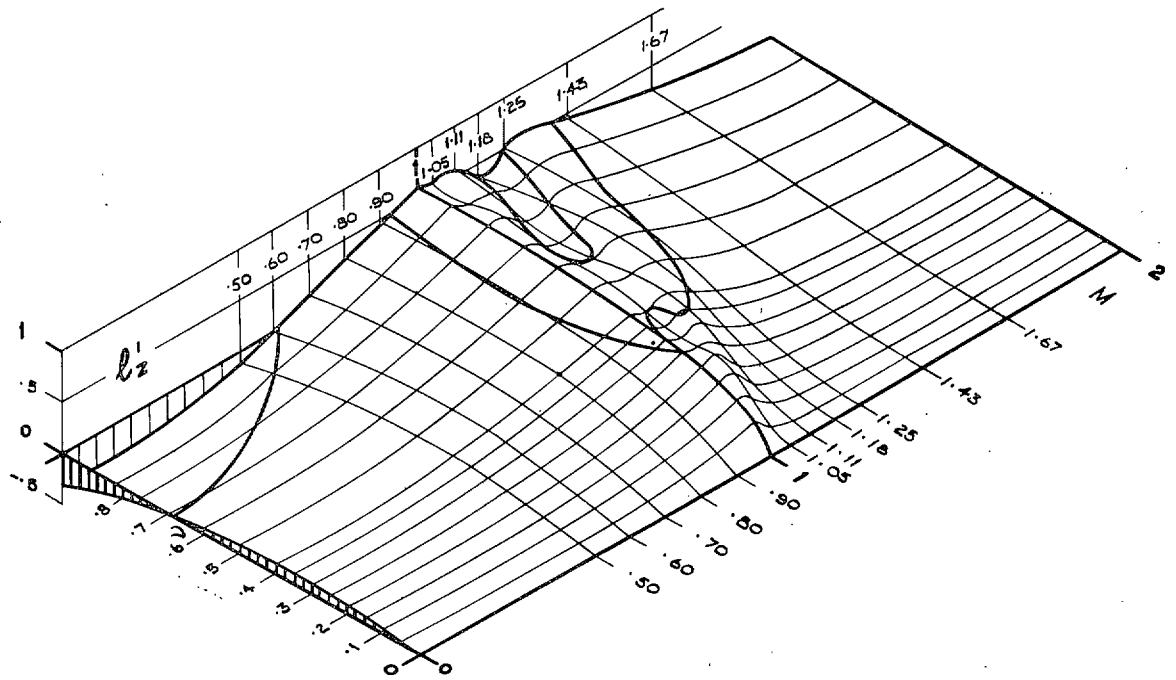


FIG. 1a. Lift coefficient  $l_z = l'_z + il''_z$ .

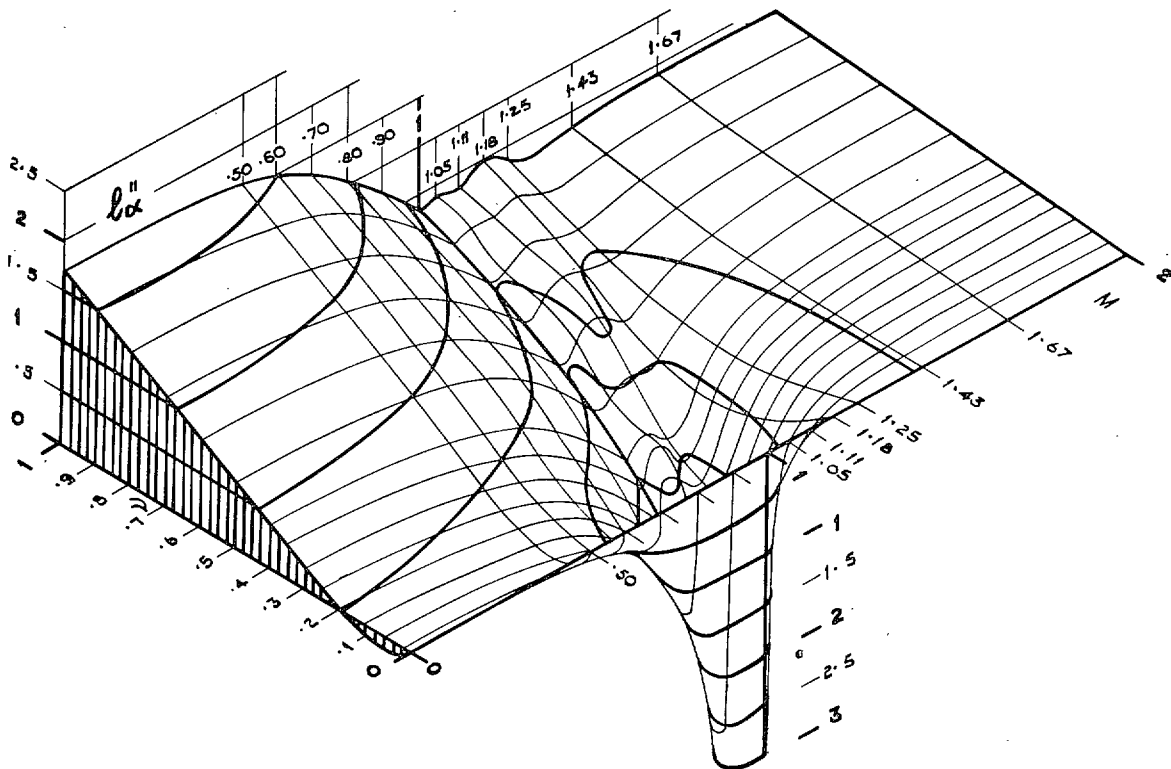
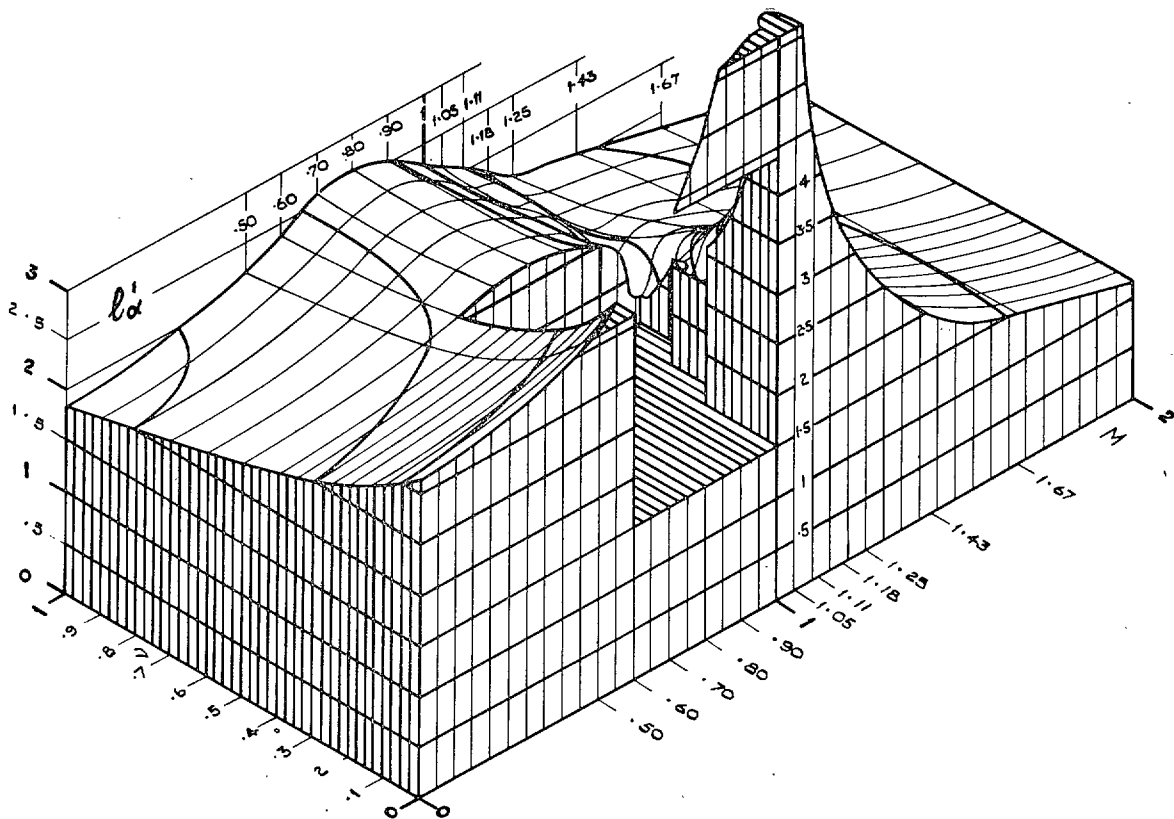


FIG. 1b. Lift coefficient  $l_\alpha$ .

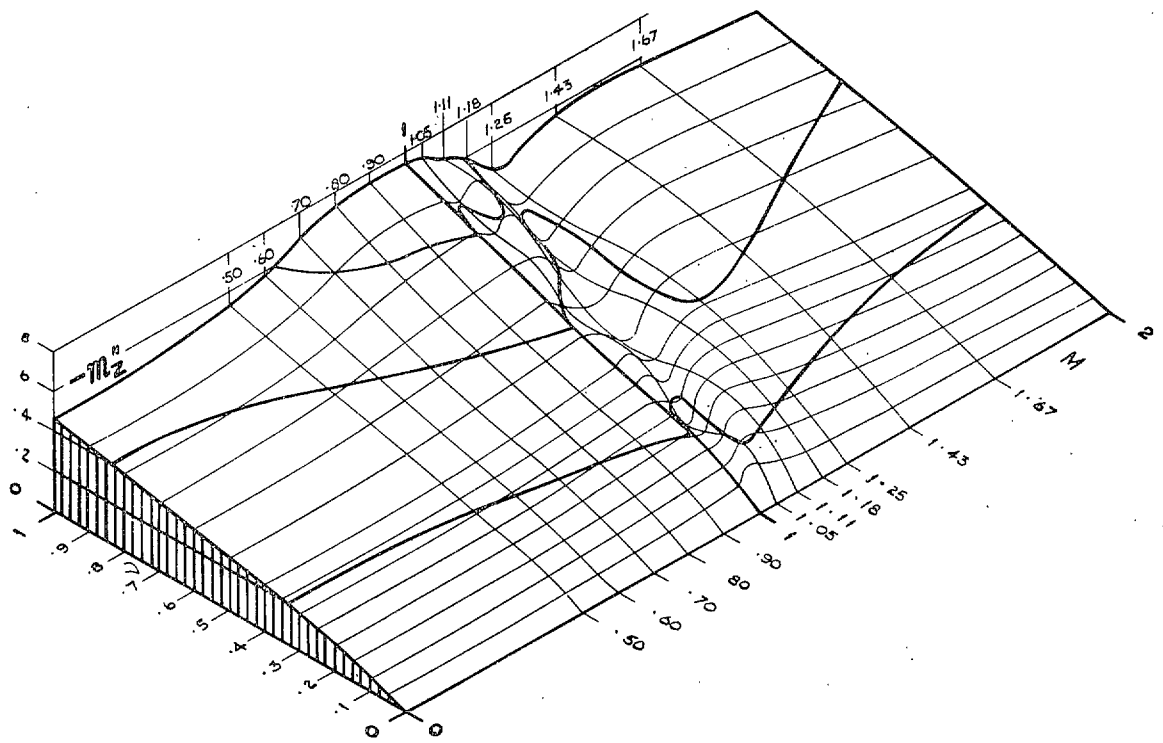
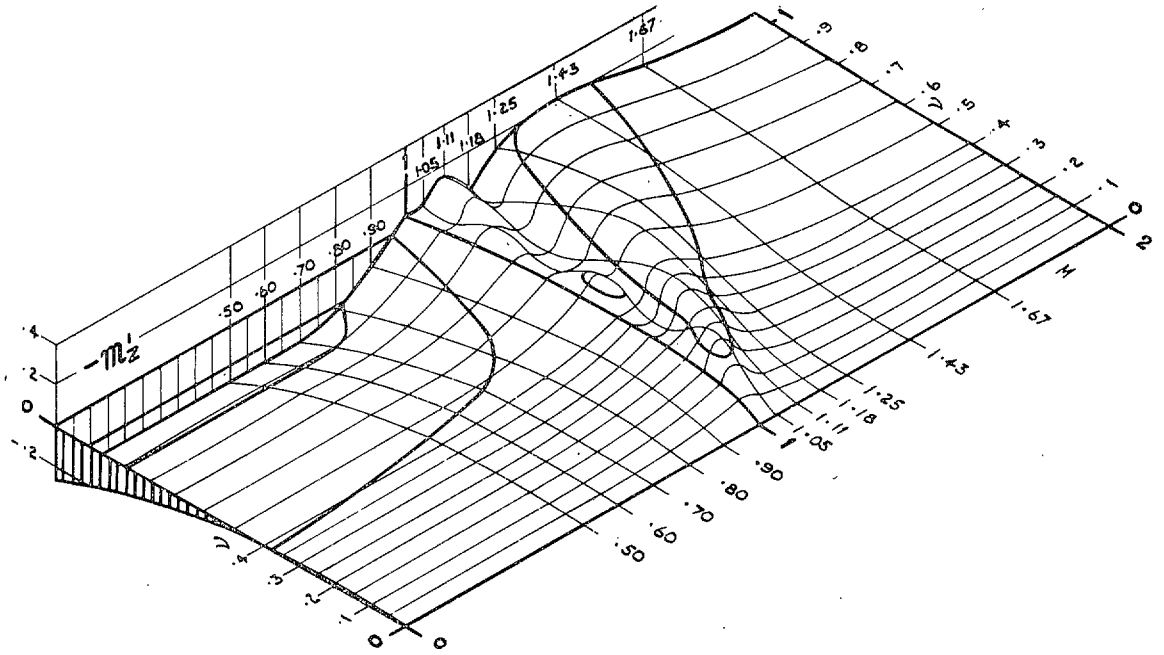


FIG. 1c. Moment coefficient  $m_z$ .

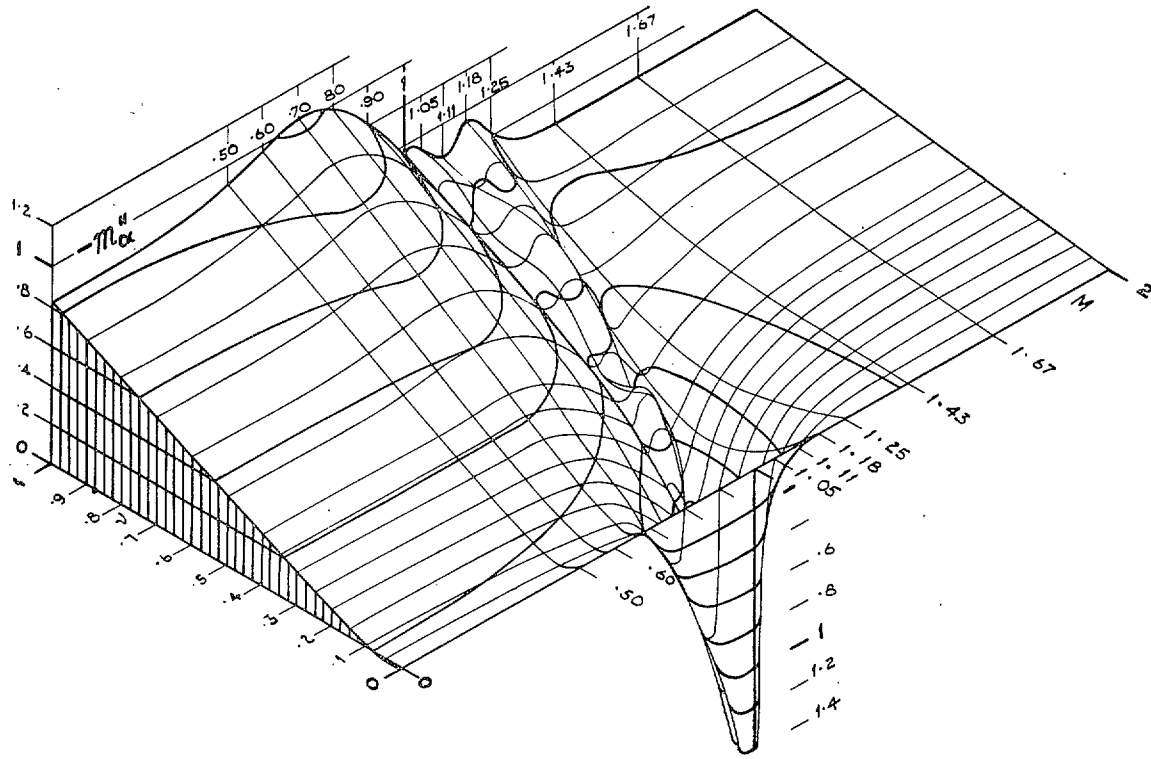
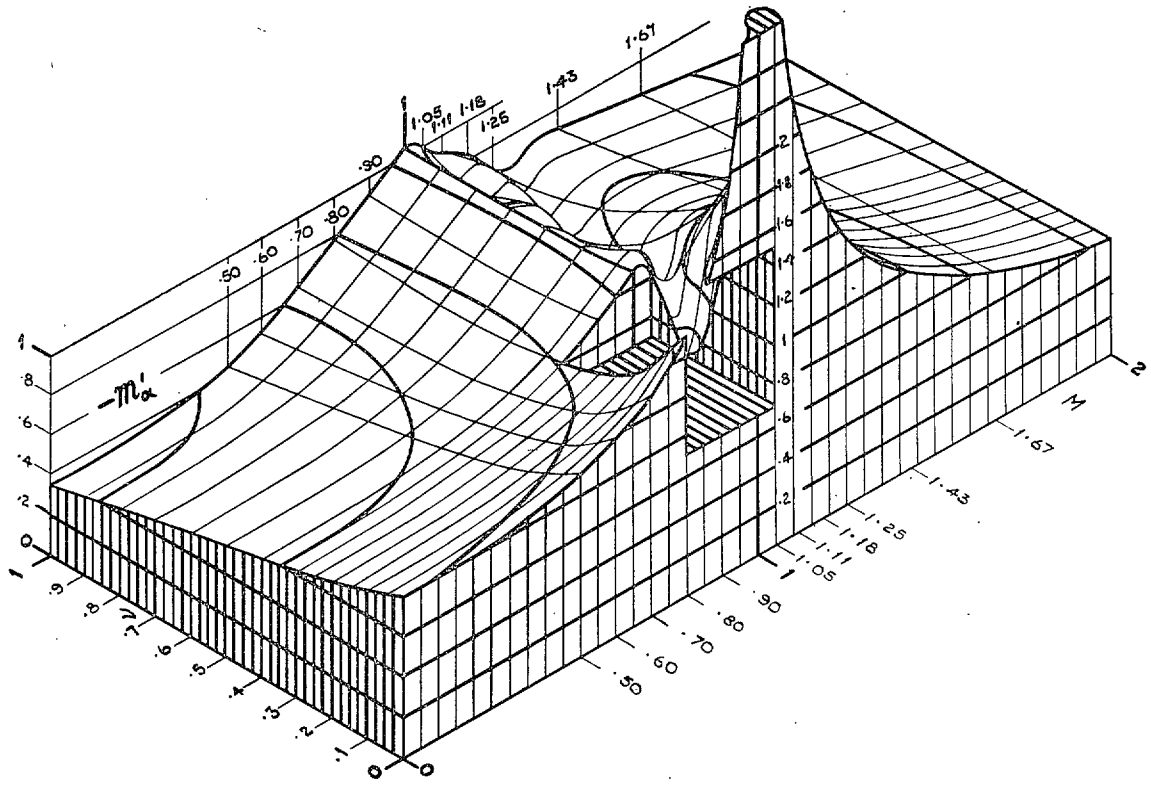


FIG. 1d. Moment coefficient  $m_{\alpha}$ .



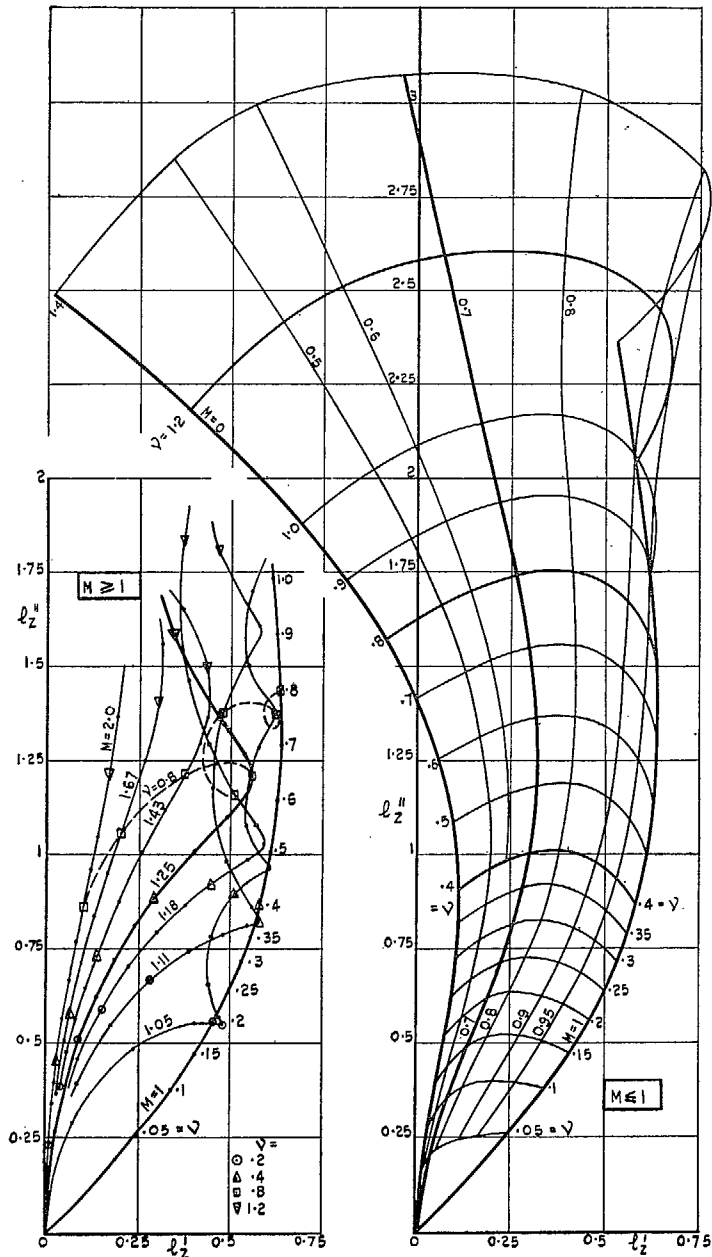


FIG. 1e.  $l_z$ . Complex presentation.

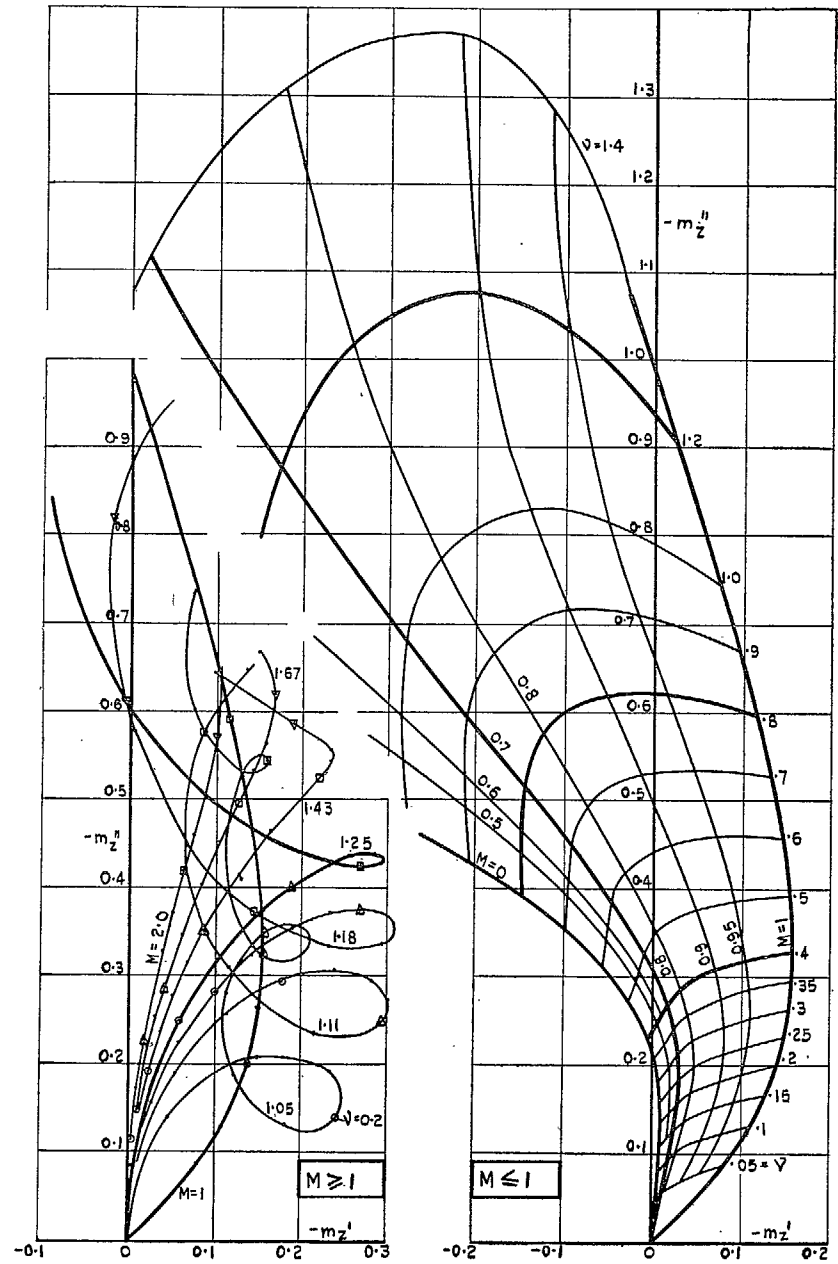


FIG. 1f.  $m_z$ . Complex presentation.

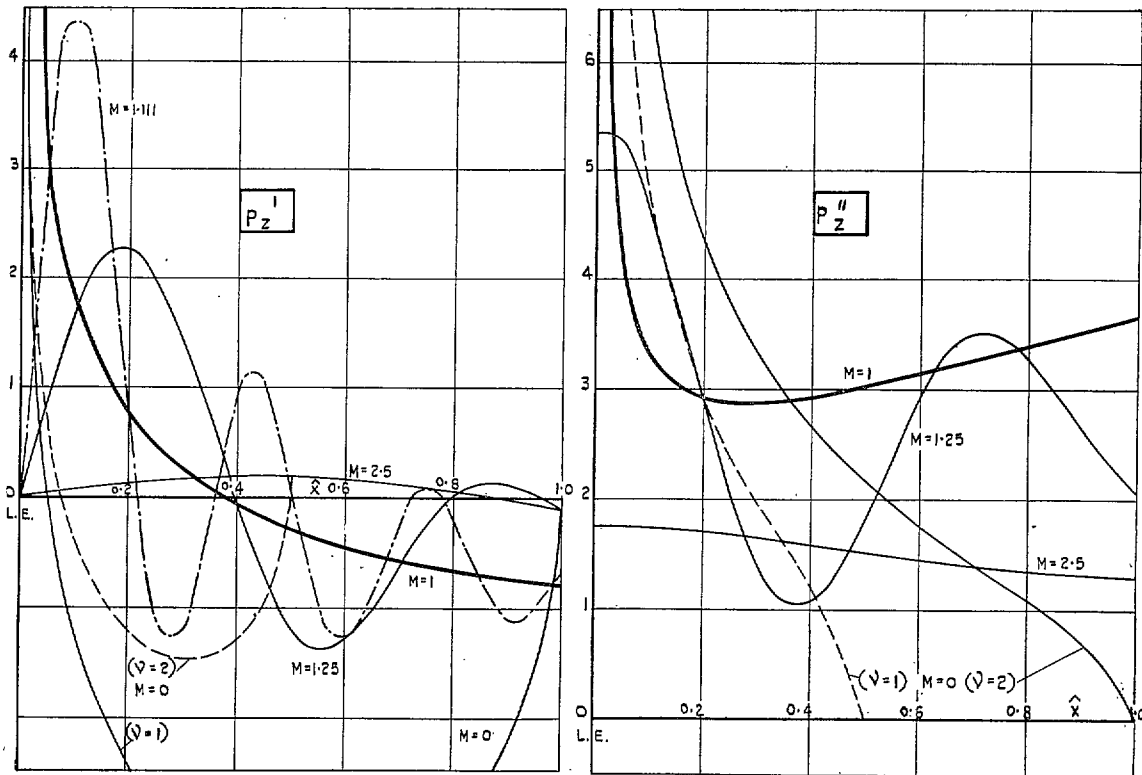


FIG. 2a. Vertical translation :  $p_z = p_z' + ip_z''$ .

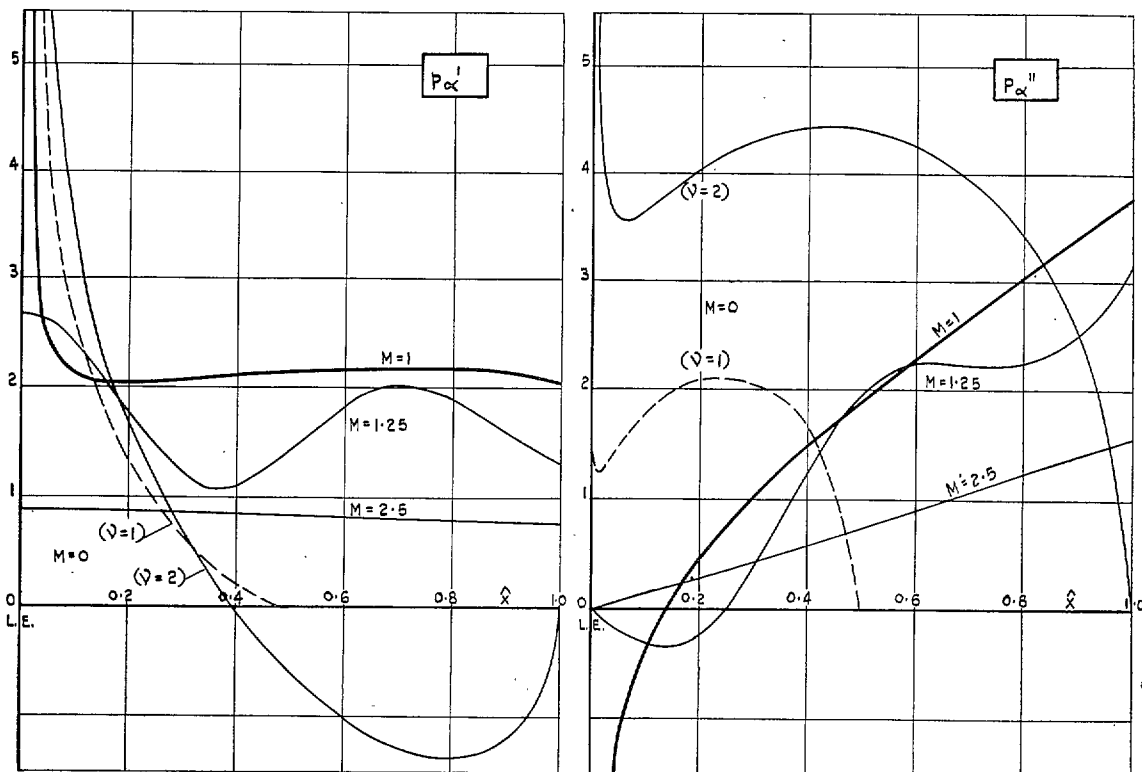


FIG. 2b. Pitching :  $p_\alpha$ .

FIG. 2. Lift distributions at different speeds.  
(See section 3.4, equation (3).)

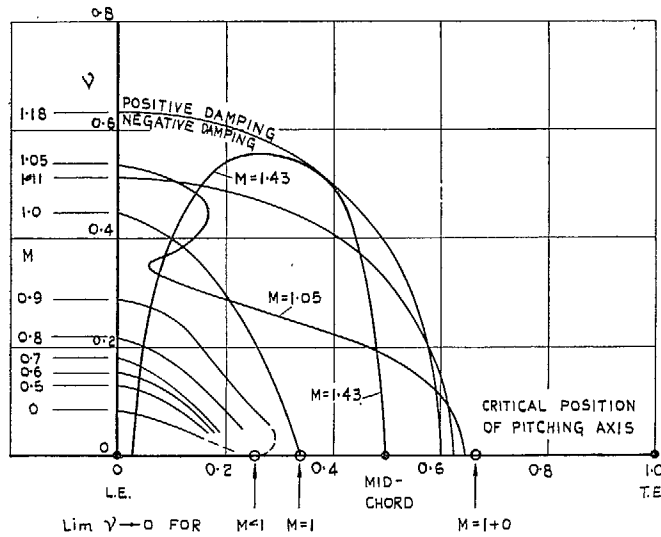


FIG. 3. Range of negative damping in pitch.

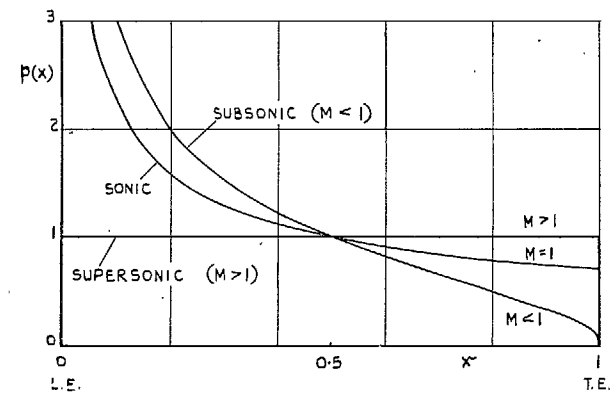


FIG. 4. Standard lift distributions  $p_0(x)$ .  
(See section 3, equation (1).)

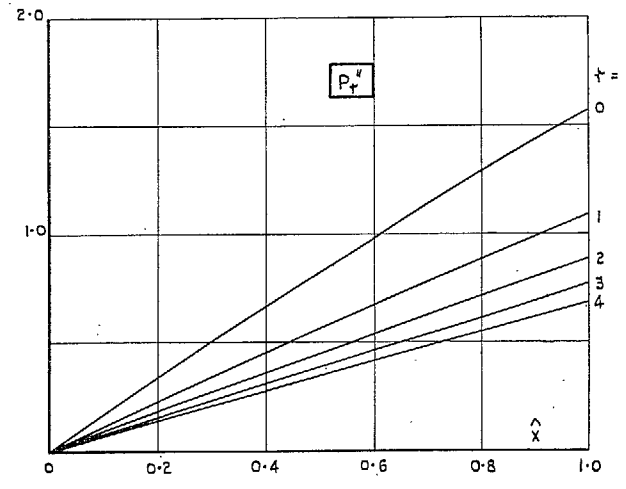
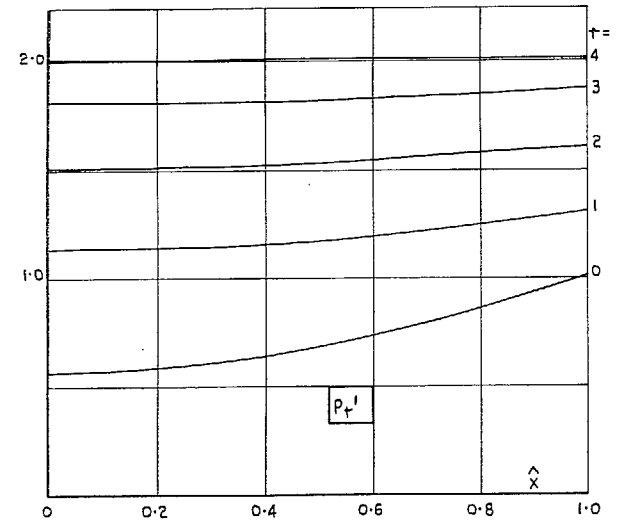


FIG. 5. Response functions  $P_+$  at sonic speed.  
(See section 3.4.2, equation (13).)

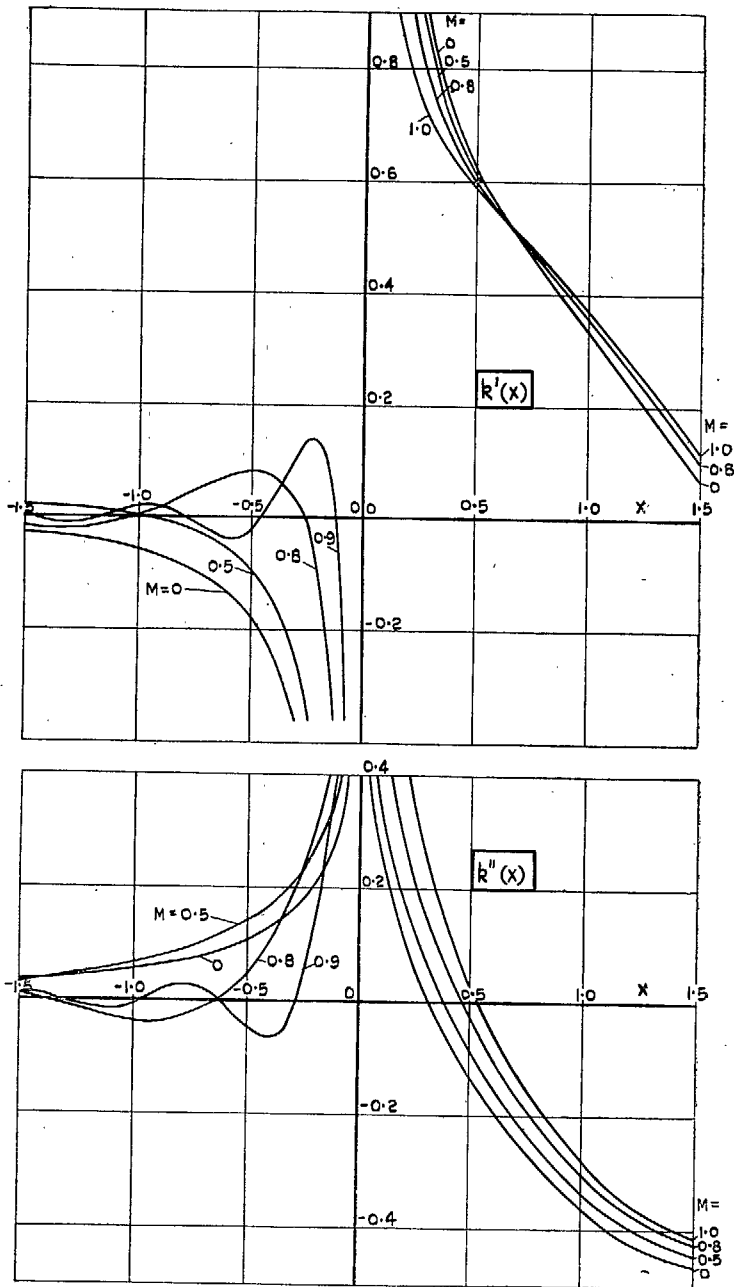


FIG. 6. Possio kernel  $k(x)$ .  
(See section 3.5.1).

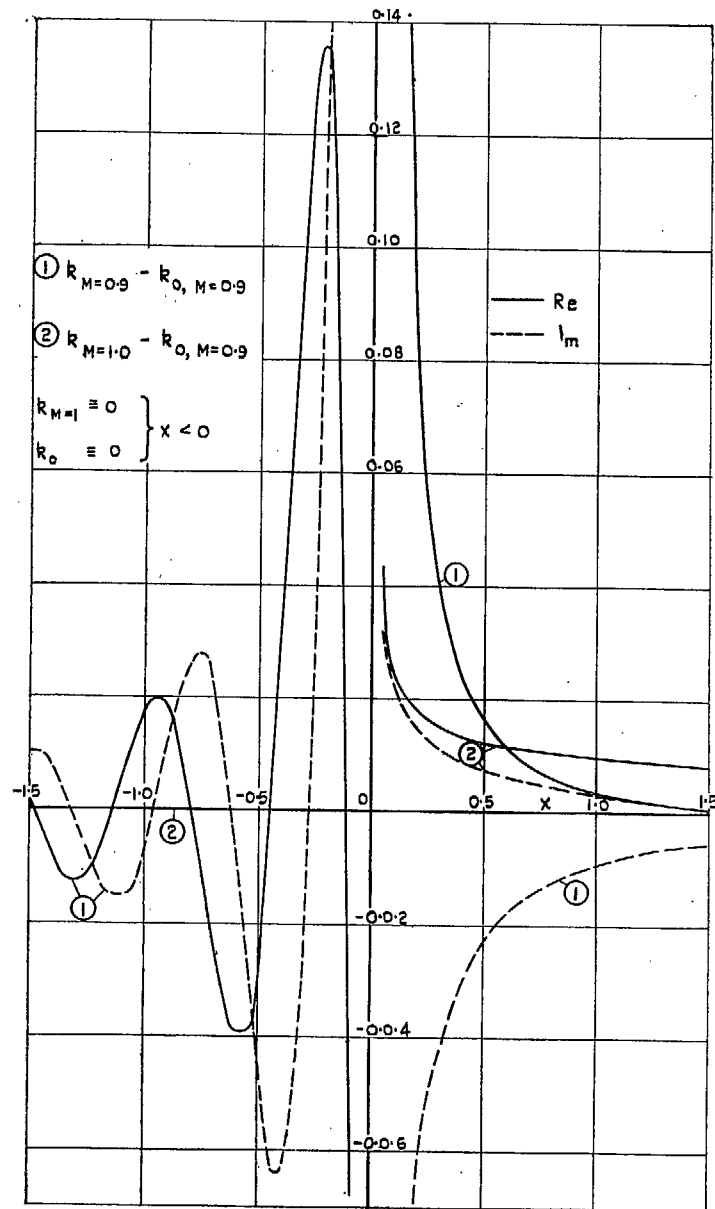


FIG. 7. Modified Possio kernel  $k_0(x)$  for  $M = 0.9$ .  
(See section 3.5.3).

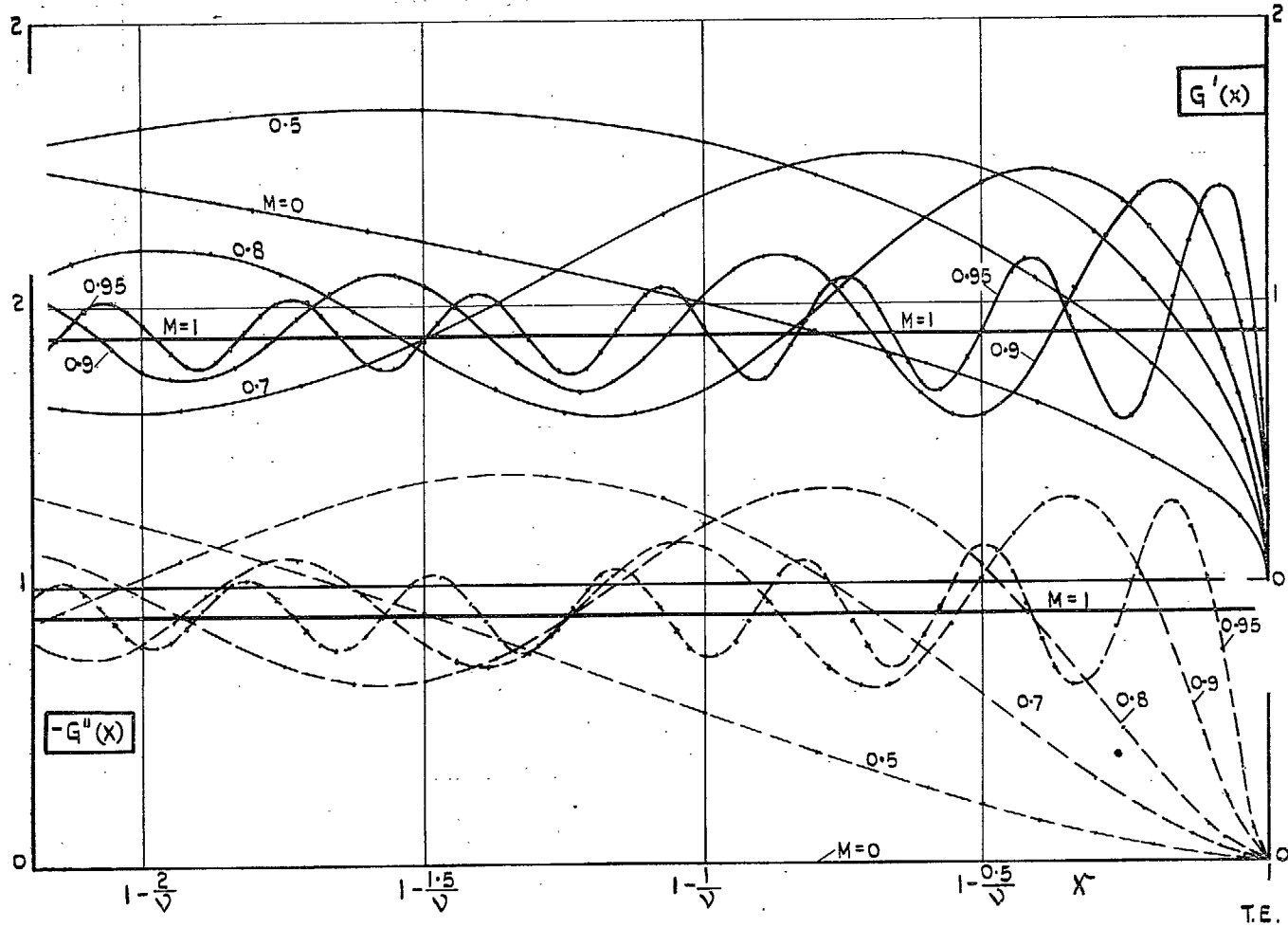


FIG. 8. Fresnel integral  $G(x) = G'(x) + iG''(x)$ .

(See section 3.5.4).

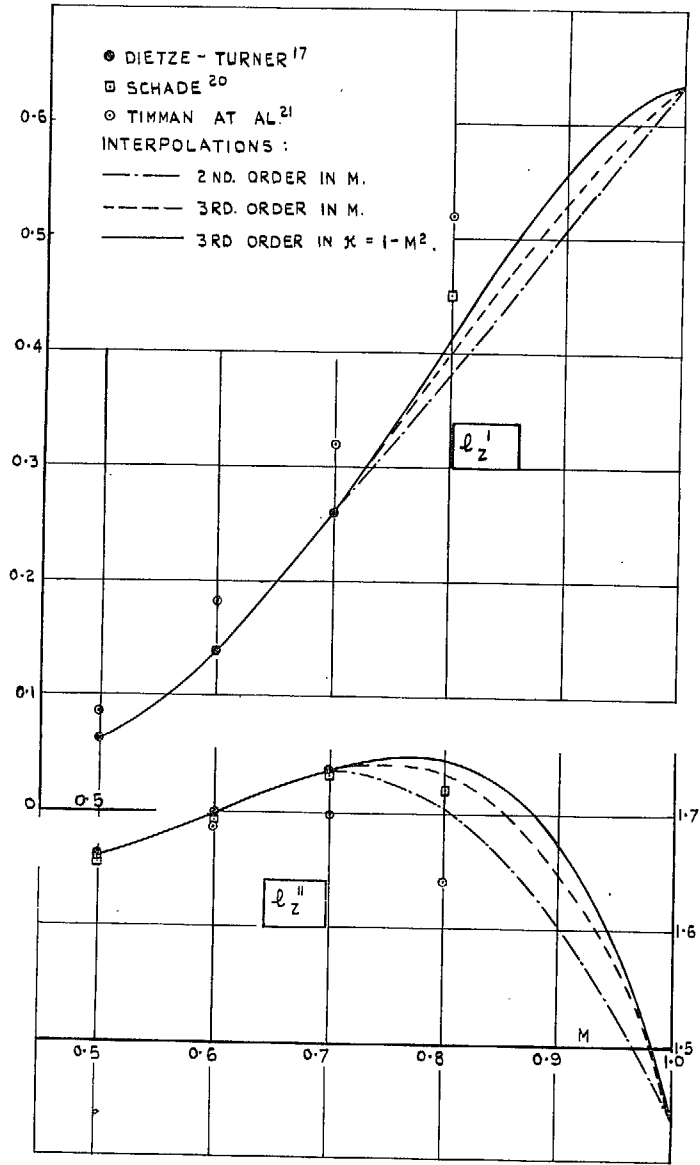


FIG. 9a. Lift coefficient  $l_z = l_z' + il_z''$ .

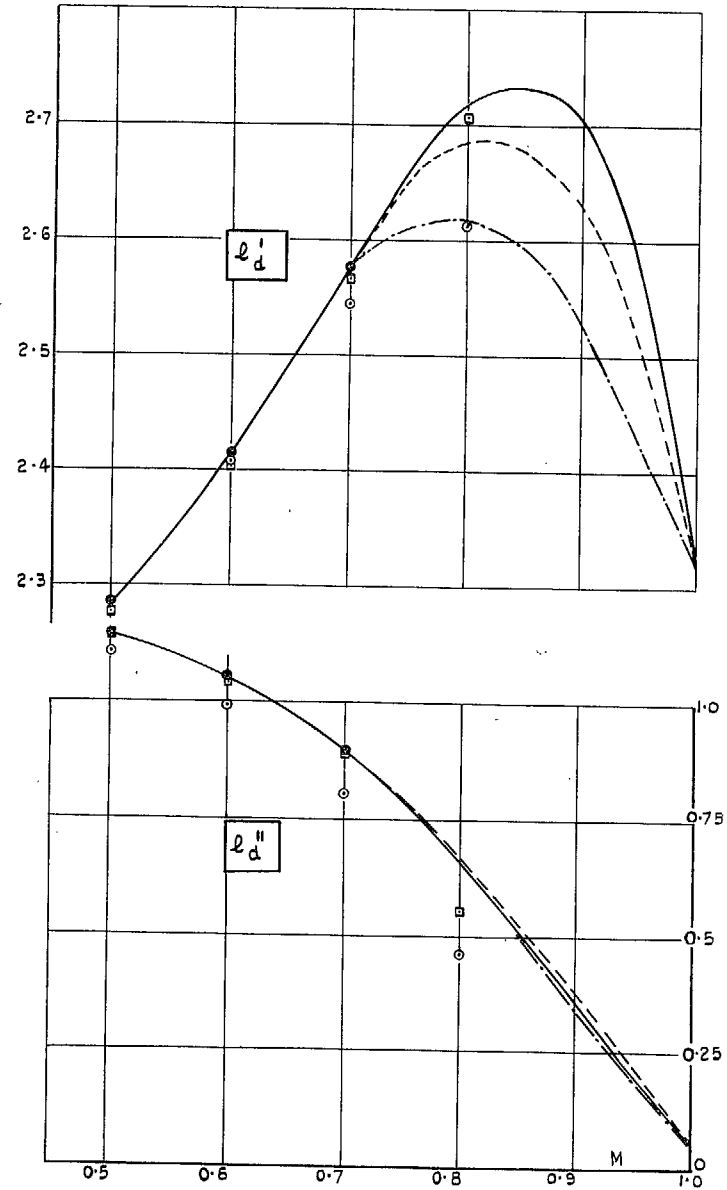


FIG. 9b. Lift coefficient  $l_\alpha$ . (For legend see Fig. 9a.)

FIGS. 9a and 9b. Different subsonic solutions and interpolations ( $\nu = 0.8$ ).

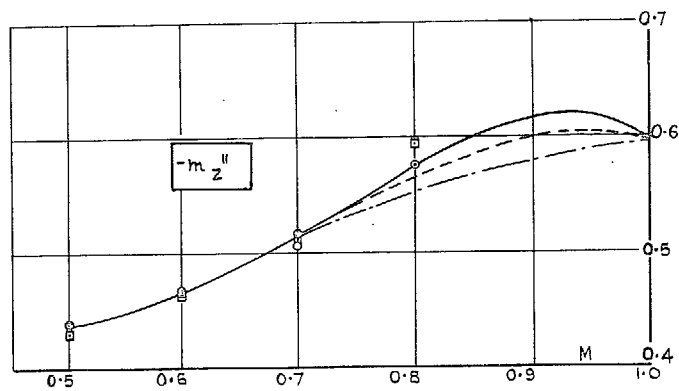
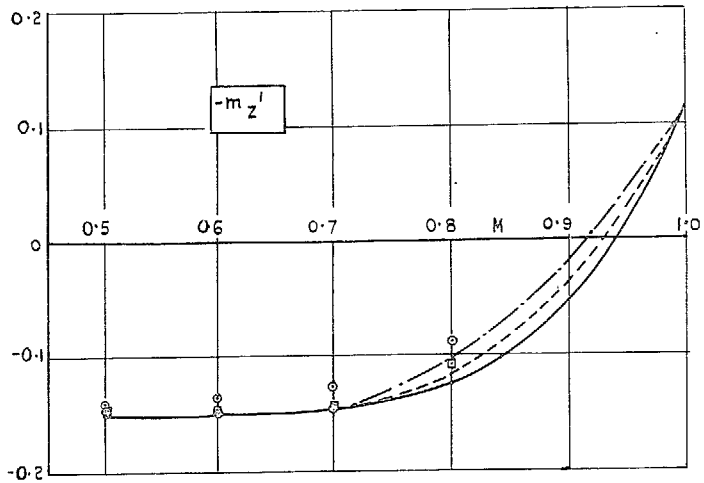


FIG. 9c. Moment coefficient  $m_z$ . (For legend see Fig. 9a.)

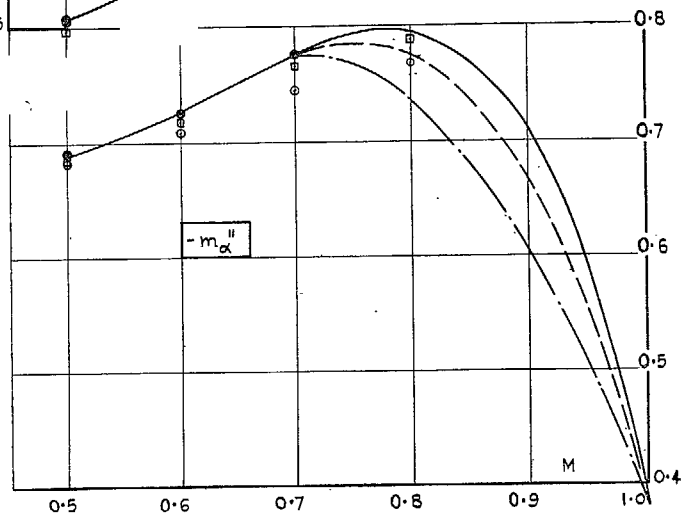
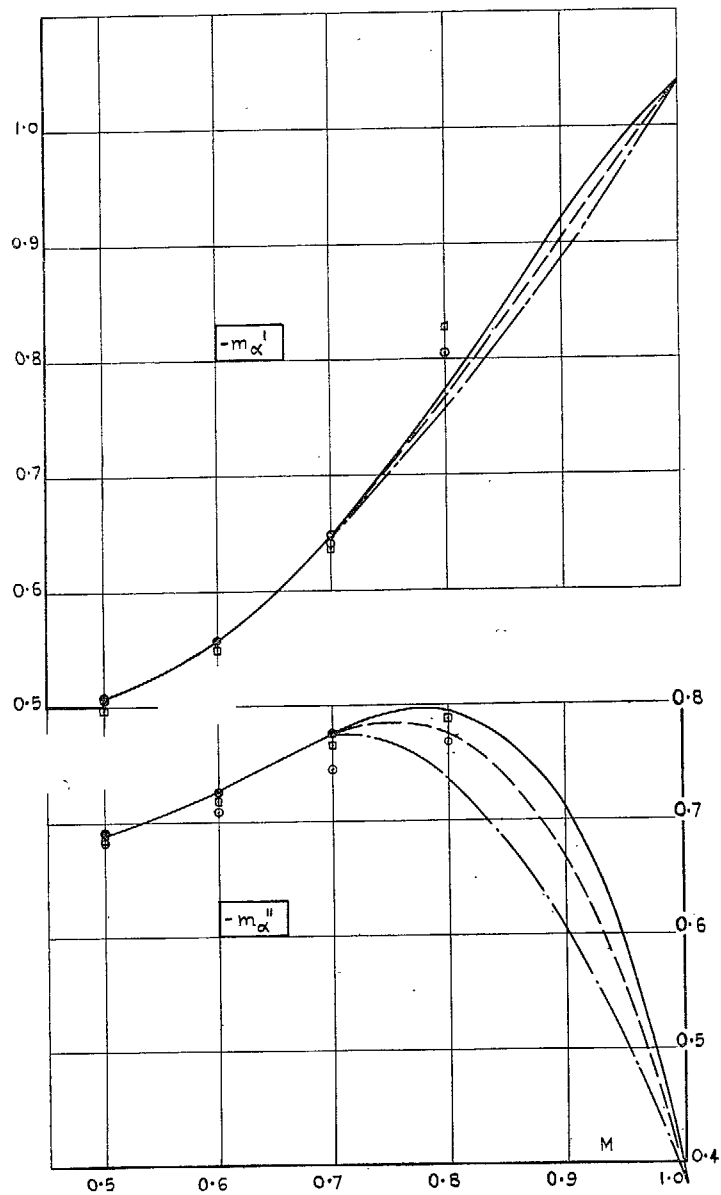


FIG. 9d. Moment coefficient  $m_\alpha$ . (For legend see Fig. 9a.)

FIGS. 9c and 9d. Different subsonic solutions and interpolations ( $\nu = 0.8$ ).

## Publications of the Aeronautical Research Council

### ANNUAL TECHNICAL REPORTS OF THE AERONAUTICAL RESEARCH COUNCIL (BOUND VOLUMES)

- 1939 Vol. I. Aerodynamics General, Performance, Airscrews, Engines. 50s. (51s. 9d.)  
Vol. II. Stability and Control, Flutter and Vibration, Instruments, Structures, Seaplanes, etc. 63s. (64s. 9d.)
- 1940 Aero and Hydrodynamics, Aerofoils, Airscrews, Engines, Flutter, Icing, Stability and Control, Structures, and a miscellaneous section. 50s. (51s. 9d.)
- 1941 Aero and Hydrodynamics, Aerofoils, Airscrews, Engines, Flutter, Stability and Control, Structures. 63s. (64s. 9d.)
- 1942 Vol. I. Aero and Hydrodynamics, Aerofoils, Airscrews, Engines. 75s. (76s. 9d.)  
Vol. II. Noise, Parachutes, Stability and Control, Structures, Vibration, Wind Tunnels. 47s. 6d. (49s. 3d.)
- 1943 Vol. I. Aerodynamics, Aerofoils, Airscrews. 80s. (81s. 9d.)  
Vol. II. Engines, Flutter, Materials, Parachutes, Performance, Stability and Control, Structures. 90s. (92s. 6d.)
- 1944 Vol. I. Aero and Hydrodynamics, Aerofoils, Aircraft, Airscrews, Controls. 84s. (86s. 3d.)  
Vol. II. Flutter and Vibration, Materials, Miscellaneous, Navigation, Parachutes, Performance, Plates and Panels, Stability, Structures, Test Equipment, Wind Tunnels. 84s. (86s. 3d.)
- 1945 Vol. I. Aero and Hydrodynamics, Aerofoils. 130s. (132s. 6d.)  
Vol. II. Aircraft, Airscrews, Controls. 130s. (132s. 6d.)  
Vol. III. Flutter and Vibration, Instruments, Miscellaneous, Parachutes, Plates and Panels, Propulsion. 130s. (132s. 3d.)  
Vol. IV. Stability, Structures, Wind tunnels, Wind Tunnel Technique. 130s. (132s. 3d.)

### ANNUAL REPORTS OF THE AERONAUTICAL RESEARCH COUNCIL—

1937 2s. (2s. 2d.)                      1938 1s. 6d. (1s. 8d.)                      1939-48 3s. (3s. 3d.)

### INDEX TO ALL REPORTS AND MEMORANDA PUBLISHED IN THE ANNUAL TECHNICAL REPORTS, AND SEPARATELY—

April, 1950 - - - - - R. & M. No. 2600. 2s. 6d. (2s. 8d.)

### AUTHOR INDEX TO ALL REPORTS AND MEMORANDA OF THE AERONAUTICAL RESEARCH COUNCIL—

1909-January, 1954 - - - - - R. & M. No. 2570. 15s. (15s. 6d.)

### INDEXES TO THE TECHNICAL REPORTS OF THE AERONAUTICAL RESEARCH COUNCIL—

December 1, 1936 — June 30, 1939. R. & M. No. 1850. 1s. 3d. (1s. 5d.)  
July 1, 1939 — June 30, 1945. - R. & M. No. 1950. 1s. (1s. 2d.)  
July 1, 1945 — June 30, 1946. - R. & M. No. 2050. 1s. (1s. 2d.)  
July 1, 1946 — December 31, 1946. R. & M. No. 2150. 1s. 3d. (1s. 5d.)  
January 1, 1947 — June 30, 1947. - R. & M. No. 2250. 1s. 3d. (1s. 5d.)

### PUBLISHED REPORTS AND MEMORANDA OF THE AERONAUTICAL RESEARCH COUNCIL—

Between Nos. 2251-2349. - - - R. & M. No. 2350. 1s. 9d. (1s. 11d.)  
Between Nos. 2351-2449. - - - R. & M. No. 2450. 2s. (2s. 2d.)  
Between Nos. 2451-2549. - - - R. & M. No. 2550. 2s. 6d. (2s. 8d.)  
Between Nos. 2551-2649. - - - R. & M. No. 2650. 2s. 6d. (2s. 8d.)

*Prices in brackets include postage*

### HER MAJESTY'S STATIONERY OFFICE

York House, Kingsway, London W.C.2; 423 Oxford Street, London W.1;  
13a Castle Street, Edinburgh 2; 39 King Street, Manchester 2; 2 Edmund Street, Birmingham 3; 109 St. Mary Street,  
Cardiff; Tower Lane, Bristol 1; 80 Chichester Street, Belfast, or through any bookseller